Protective effects of CXCR3/HO-1 gene-modified BMMSCs on damaged intestinal epithelial cells: Role of the p38-MAPK signaling pathway

MINGLI YIN[1*], ZHONGYANG SHEN[2,3*], LIU YANG[1], WEIPING ZHENG[2,4] and HONGLI SONG[2,5]

[1]Tianjin First Central Hospital Clinic Institute, Tianjin Medical University, Tianjin 300070; [2]Department of Organ Transplantation, Tianjin First Central Hospital; [3]Tianjin Clinical Research Center for Organ Transplantation; [4]Key Laboratory of Emergency and Care Medicine of Ministry of Health; [5]Tianjin Key Laboratory of Organ Transplantation, Tianjin 300192, P.R. China

Received August 13, 2018; Accepted February 27, 2019

DOI: 10.3892/ijmm.2019.4120

Abstract. The purpose of the present study was to investigate whether bone marrow mesenchymal stem cells (BMMSCs) modified by CXC-chemokine receptor type 3 (CXCR3) and heme oxygenase-1 (HO-1) genes can repair damaged intestinal epithelial cells *in vitro*, and the role of the p38 mitogen-activated protein kinase (p38-MAPK) pathway in this process. A model of intestinal epithelial crypt cell line-6 (IEC-6) damage was created, and BMMSCs were transfected with either the CXCR3 and/or HO-1 gene *in vitro*. There were nine experimental groups in which the damaged IEC-6 cells were co-cultured with differentially-treated BMMSCs and lymphocytes for 24 h. Reverse transcription-quantitative polymerase chain reaction analysis, immunohistochemistry and a western blot analysis were performed to detect stem cell transfection, the repair of damaged intestinal epithelial cells and the expression of related molecules in the P38-MAPK pathway, respectively. Crystal violet staining and live cell imaging were used to detect the chemotaxis of BMMSCs. Flow cytometry was used to detect T lymphocyte activity and the surface markers expressed on BMMSCs. An ELISA was used to quantify cytokine production. The adenovirus (Ad)-CXCR3/MSCs exhibited the characteristics of stem cells and exhibited chemotaxis. The Ad-CXCR3/MSCs and Ad-(CXCR3 + HO)/MSCs exhibited increased expression of tight junction protein zonula occludens-1 (ZO-1) and anti-proliferating cell nuclear antigen in the damaged IEC-6 cells, and apoptosis of the damaged IEC-6 cells was decreased. BMMSCs inhibited the phosphorylation of p38, in addition to downstream molecules of the p38MAPK signaling pathway. The Ad-CXCR3/MSCs and Ad-(CXCR3 + HO)/MSCs exhibited significantly decreased expression levels of downstream molecules, including phosphorylated (p)-p38, p-activated transcription factor 2, p-C/EBP homologous protein-10, and p-myocyte enhancer factor 2C, and target molecules (e.g., apoptotic bodies). The effects of Ad-(CXCR3 + HO)/MSCs on the repair of the damaged intestinal tract and inhibition of the p38-MAPK pathway was more marked than those in other groups on day 7 post-surgery in the rejection model for small bowel transplantation. BMMSCs modified by the CXCR3 and HO-1 genes exhibited superior ability to repair damaged intestinal epithelial cells and served this role via the p38-MAPK pathway.

Correspondence to: Professor Hongli Song, Department of Organ Transplantation, Tianjin First Central Hospital, 24 Fukang Road, Nankai, Tianjin 300192, P.R. China
E-mail: hlsong26@163.com

*Contributed equally

Abbreviations: CXCR3, CXC-chemokine receptor CXCR3; BMMSCs, bone marrow mesenchymal stem cells; HO-1, heme oxygenase-1; IEC-6, intestinal epithelial crypt cell line-6; TNF-α, tumor necrosis factor-α; GFP, green fluorescence protein; p38-MAPK, p38 mitogen activated protein kinase; p-CHOP10, anti-phosphorylated-C/EBP homologous protein-10; p-MLK3, phosphorylated-mixed lineage kinases 3; p-MKK3, phosphorylated-mitogen-activated protein kinase kinase 3; p-MEF2C, phosphorylated-myocyte enhancer factor type 2C; IFN-γ, interferon-γ; IL-2, interleukin-2

Key words: bone marrow mesenchymal stem cells, CXC-chemokine receptor type 3, heme oxygenase-1, intestinal epithelial cells, p38-mitogen-activated protein kinase signaling pathway, repair mechanism

Introduction

Small bowel transplantation is the most effective treatment of intestinal failure (1); however, the high incidence of intestinal tissue injury, and the risk of acute and chronic rejection following transplantation are difficulties associated with small bowel transplantation (2). Although the development of novel immunosuppressive agents has reduced the incidence of rejection and significantly prolonged the survival of grafts, damage to function and the poor postoperative recovery of intestinal epithelial cells remain problems that require

urgent resolution (3). Previous studies have found that bone marrow mesenchymal stem cells (BMMSCs) are able to repair damaged cells or tissues (4,5), with obvious biological and ethical advantages (6,7), and is a potential cellular source for cell therapy strategies (8). In addition, animal experiments have demonstrated that the transfusion of BMMSCs following small bowel transplantation can significantly improve the function and repair the damage of the transplanted intestinal tract (9). However, the viability of BMMSCs and their capacity to home to lesions following transfusion into the recipient are limited (10), and the majority of the cells die within a few hours (11) even if the BMMSCs were transfused into the local lesion site. Heme oxygenase-1 (HO-1) and its metabolites have been found to exhibit anti-oxidative, anti-inflammatory, antiproliferative and immunomodulatory effects (12). Transfection with HO-1 can improve the transformation and anti-oxidative capacity of BMMSCs (13), thereby enhancing the activity of BMMSCs and prolonging the duration in which BMMSCs serve a role (14).

CXC-chemokine receptor 3 (CXCR3) is a G protein-coupled seven-subunit transmembrane receptor expressed in damaged parenchymal cells in lesions from multiple organs, and in inflammatory cells, including activated lymphocytes, macrophages and dendritic cells (15). CXCR3 receptors bind to their specific ligands [monokine induced by interferon (IFN)-γ, IFN-γ-inducible protein 10 and IFN-γ-inducible T-cell α chemoattractant], and recruit CXCR3-expressing cells to the site of injury (16,17). It has been shown that, following transfection with the CXCR3 gene, BMMSCs are chemotactically directed to migrate to a transplanted intestine; this was shown by the increased homing of BMMSCs and inhibited chemotaxis of T cells to transplanted intestine, resulting in protective effects on the transplanted small bowel (18). In our preliminary study, HO-1 and CXCR3 genes were transfected into BMMSCs *in vitro*, and subsequently transfused into a rat model of rejection to small bowel transplantation. The results showed that the HO-1 and CXCR3 gene-modified BMMSCs were significantly increased in the damaged sites, and the function of the damaged intestine quickly recovered (18). However, the mechanism by which the recovery of intestinal function was achieved remains to be elucidated and requires further investigation.

It has been found that mitogen-activated protein kinases (MAPKs) are important intracellular signal transduction systems that serve an important role in the development of inflammatory responses (19) induced by trauma (20), infection (21) and ischemia-reperfusion (22). The activation of the p38-MAPK pathway is important in cellular damage, including the production of proinflammatory cytokines, cytoskeletal remodeling and cellular apoptosis (23). However, whether the p38-MAPK signaling pathway is involved in the recovery of transplanted intestinal function by BMMSCs has not been reported. In addition, tumor necrosis factor (TNF)-α has been shown to be involved in the recovery of transplanted intestinal function by CXCR3/HO-1 gene-modified BMMSCs in rats (18). The rat intestinal epithelial crypt cell line-6 (IEC-6) cell line is derived from the intestinal crypt of normal rats, which can be applied to the *in vitro* investigation of intestinal mucosal injury (24). Therefore, in the present study, an *in vitro* model of damaged intestinal epithelial cells was established using IEC-6 cells treated with TNF-α to investigate the effects of CXCR3/HO-1 gene-modified BMMSCs on intestinal epithelial cell damage.

Materials and methods

Acquisition and transfection of BMMSCs. All animals were provided by the Experimental Animal Center of the Academy of Military Medical Sciences (Beijing, China) and were housed individually in standard animal facilities at 18-26˚C and 40-70% relative humidity with a 12-h light/dark cycle, and were provided with commercially available chow and tap water *ad libitum*. All experiments involving animals followed the experimental animal ethical regulations, and were approved by the Ethics Committee of Tianjin First Central Hospital (Tianjin, China). Healthy male Lewis rats (n=15) aged 2-3 weeks and weighing 40-60 g were sacrificed by cervical dislocation and soaked in 75% alcohol for 5-10 min. The bone marrow cells were cultured in DMEM-F12 (Gibco; Thermo Fisher Scientific, Inc., Waltham, MA, USA) medium containing 10% fetal bovine serum (FBS; Biowest, Loire Valley, France) and the third generation of the cultured cells was prepared for further use (18). The third generation BMMSCs were induced to differentiate into adipocytes and osteoblasts, and subjected to phenotypic assessment (25). The third generation BMMSCs were inoculated into a 75-mm culture flask with $5x10^6$ cells/flask containing 20 ml complete medium (DMEM-F12 containing 10% FBS). The culture solution was discarded following culture for 24 h. Subsequently, 5 ml of each culture medium was added to the different BMMSC groups as follows: MSCs with culture medium only; Ad/MSCs with medium containing adenovirus; Ad-HO/MSCs with medium containing the HO-1 transgene; Ad-CXCR3/MSCs with medium containing the CXCR3 transgene; Ad-(CXCR3 + HO)/MSCs with medium containing the HO-1 and CXCR3 transgenes (all Shanghai Genechem Co., Ltd.). The BMMSC to transgene ratio was 1:10 (MOI=10). Following incubation for 6 h, the medium containing the transfection solution was discarded and 20 ml complete medium was added for 48 h. Fluorescent protein expression was observed under a fluorescence microscope (Nikon Corporation, Tokyo, Japan,) in the dark. These cells were used in subsequent experiments.

In vitro model of intestinal cell damage. The IEC-6 cells (National Infrastructure of Cell Line Resource, Beijing, China) were inoculated in a six-well plate at a density of $2x10^5$ cells/well. After 24 h, the culture medium was discarded, and the IEC-6 cells were cultured in complete RPMI-1640 medium containing 10% FBS (Gibco; Thermo Fisher Scientific, Inc.) and 100 ng/ml TNF-α (PeproTech, Inc., Rocky Hill, NJ, USA) for 48 h to establish the model of damaged IEC-6 cells (TNF-α/IEC-6) (26). Rat lymphocytes were obtained using the method described by Yin *et al* (18).

The cells were divided into nine experimental groups: i) Control group, untreated IEC-6 cells; ii) Model group, TNF-α/IEC-6; iii) L group, TNF-α/IEC-6 + lymphocytes; iv) S + L group, p38 inhibitor + TNF-α/IEC-6 + lymphocytes; v) MSCs + L group, BMMSCs + TNF-α/IEC-6 + lymphocytes; vi) Ad/MSCs + L group, Ad/BMMSCs + TNF-α/IEC-6 + lymphocytes;

vii) Ad-HO/MSCs + L group, Ad-HO-1/BMMSCs + TNF-α/IEC-6 + lymphocytes; viii) Ad-CXCR3/MSCs + L group, Ad-CXCR3/BMMSCs + TNF-α/IEC-6 +lymphocytes; and ix) Ad-(CXCR3 + HO)/MSCs + L group, Ad-(CXCR3 + HO-1)/BMMSCs + TNF-α/IEC-6 + lymphocytes. The TNF-α/IEC-6 cells were prepared in the lower Transwell (Corning Inc., Corning, NY, USA) layer, whereas the BMMSCs ($1x10^6$ cells/well) and lymphocyte ($5x10^6$ cells/well) were added to the upper layer of the Transwell chamber. The cells were co-cultured for 24 h and then collected following the experiment.

Chemotaxis. The experimentally-treated Transwell chambers were fixed (anhydrous methanol: Glacial acetic acid 3:1) for 30 min, stained with a 2% crystal violet dye solution for 30 min and washed with phosphate-buffered saline (PBS). The upper layer of cells was removed with a cotton swab, peeled off and placed on a slide, fixed with neutral gum, and then observed under a Ti2-E inverted microscope, (Nikon Corporation). The TNF-α/IEC-6 cells were prepared in a 35-mm diameter well and added to a Transwell chamber containing Ad/MSCs, Ad-CXCR3,/MSCs or Ad-(CXCR3 + HO)/MSCs. The green fluorescent protein (GFP) signal was locked with a living cell workstation microscope, and GFP-expressing BMMSCs located 5 μm below the Transwell membrane were observed to record the time at which when BMMSCs began to appear.

Cell viability. The BMMSCs and IEC-6 cells in each of the groups were trypsinized and adjusted to a density of $1x10^5$ cells/ml. To each well, 200 μl of the cell suspension was added according to the different groups, and 200 μl complete medium containing 10% FBS was added to the blank control wells. The cells were incubated at 37˚C for 24 h, following which 10 μl of the CCK-8 solution (Dojindo Molecular Technologies, Inc., Kumamoto, Japan) was added to each well. Following culture for 3 h, the absorbance was measured at 450 nm with an enzyme standard instrument (BioTek Synergy 2, BioTek Instruments, Inc., Winooski, VT, USA) to calculate the cellular viability.

Immunohistochemistry. Third passage BM MSCs were placed into six-well plates containing a cell slide, at a density of $2.5x10^5$ cells/well. After 24 h, transfection was performed, and different BMMSCs were obtained. The culture solution was discarded, the BMMSCs were washed with PBS, fixed with 4% paraformaldehyde for 30 min, washed with PBS, and treated with 1% NP40 (both Beijing Solarbio Science and Technology Co., Ltd., Beijing, China) for 30 min to rupture the cell membrane. Following washing with PBS and blocking with 10% goat serum (Minghai, Lanzhou, China) for 30 min, each slide was then stained with a mixture of anti-HO-1 mouse IgG (1:100; cat. no. ab13248; Abcam, Cambridge, UK) and anti-CXCR3 rabbit IgG (1:100; cat. no. bs-2209R; Affinity Bioreagents, Inc., Golden, CO, USA) at 4˚C overnight. Following allowing the slides to recover to room temperature for 30 min and washing via dipping in PBS, all slides were stained with a secondary antibody mixture of Alexa Fluor 594 (1:100; cat. no. ZF-0513; OriGene Technologies, Inc., Beijing, China)-conjugated goat anti-mouse IgG and Alexa Fluor 488-conjugated goat anti-rabbit IgG (1:100; cat. no. ZF-0511; OriGene Technologies, Inc.). The slides were incubated at 37˚C for 1 h, washed with PBS, stained with 4',6-diamidino-2-phenylindole (10 μg/ml; Beijing Solarbio Science and Technology Co., Ltd.) for 2 min, rinsed with running water, and observed under a laser confocal microscope (Nikon Corporation). The IEC-6 cells were cultured on the slide in advance, and different IEC-6 groups were obtained following exposure to different treatments. The steps were the same as above, and the slides were stained separately with the following antibodies: Anti-zonula occludens-1 (ZO-1) rabbit IgG (1:100; cat. no. 21773-1-AP; ProteinTech Group, Inc., Chicago, IL, USA), followed by Alexa Fluor 488-conjugated goat anti-rabbit IgG (1:50), or the anti-phosphorylated (p)-C/EBP homologous protein-10 (p-CHOP10) rabbit IgG (1:100; cat. no. bs-51772; BIOSS, Beijing, China), followed by secondary Alexa Fluor 594-horseradish peroxidase (HRP)-conjugated goat anti-rabbit IgG (1:50). Staining of apoptosis was performed for each IEC-6 group using TUNEL kits (Roche Diagnostics, Basel, Switzerland) according to the manufacturer's protocol.

The paraffin-fixed small intestine tissues were immunohistochemically stained. The tissue sections were incubated at 70˚C for 50 min, deparaffinized with xylene, hydrated with gradient alcohol, and citrated for 15 min at 95˚C, and then blocked with goat serum for 1 h. The paraffin sections were stained with anti-p-CHOP10 rabbit IgG (1:100) overnight at 4˚C. Following incubation at room temperature for 30 min, the sections were stained with HRP (Thermo Fisher Scientific, Inc.) for 1 h at 37˚C. Following DAB staining, hematoxylin counterstaining, alcohol dehydration and transparency, the tissue sections were fixed with neutral gum and were observed under the Eclipse Ni-U positive fluorescence microscope (Nikon Corporation).

Western blot analysis. The BMMSCs from each of the groups were exposed to 500 μl RIPA lysis buffer on ice for 30 min. Following centrifugation at 13,000 x g for 5 min at 4˚C, the supernatant was obtained to assess the concentrations of various proteins. Protein determination was performed using a bicinchoninic acid assay (Wuhan Boster Biological Technology, Ltd., Wuhan, China). SDS-PAGE (10%) was used for HO-1 and CXCR3. A total of 30 μg proteins/well in the gels underwent electrophoresis, and were transferred onto a nitrocellulose membrane (Beijing Solarbio Science and Technology Co., Ltd.) and blocked with skimmed milk (BD Biosciences, Franklin Lakes, NJ, USA) for 2 h at room temperature, following which the membranes were stained with anti-HO-1 mouse IgG (1:400) or anti-CXCR3 rabbit IgG (1:800) or β-actin rabbit IgG (1:2,000; cat. no. 21338; SAB, College Park, Maryland, United States) at 4˚C overnight. The membranes were washed three times with TBST, stained with goat anti-rabbit IgG (1:1,000; cat. no. zb2301) or goat anti-mouse IgG (1:1,000; cat. no. zb2305; both OriGene Technologies, Inc.), and incubated at room temperature for 2 h. Following treatment with a developing solution (EMD Millipore, Billerica, MA, USA) the membranes were exposed (ProteinSimple, San Jose, CA, USA), the expression levels of HO-1 and CXCR3 in the different groups was calculated using a relative quantitative analysis method using Alphaview SA software 3.4.0.0 (ProteinSimple). The IEC-6 cells in the different groups and transplanted small bowel on day 7 post-transplantation were collected for protein extraction using the same steps as those described above. The primary

antibodies used were as follows: Anti-GAPDH rabbit IgG (1:2,000; cat. no. 21612; SAB), anti-proliferating cell nuclear antigen (PCNA) mouse IgG (1:500; cat. no. EM111201; Abcam), anti-ZO-1 rabbit IgG (1:1,000), anti-p-mixed lineage kinases 3 (p-MLK3) rabbit IgG (1:800; cat. no. ab191530; Abcam), anti-MLK3 rabbit IgG (1:500; cat. no. 11996-1-AP; ProteinTech Group, Inc.), anti-p MAPK kinase 3 (p-MKK3) rabbit IgG (1:1,000; cat. no. 12280; Abcam), anti-MKK3 rabbit IgG (1:500; cat. no. 13898-1-AP; ProteinTech Group, Inc.), anti-p-p38 rabbit IgG (1:800; cat. no. ab47363; Abcam), anti-p38 rabbit IgG (1:500; cat. no. 9212S; Cell Signaling Technology, Inc., Danvers, MA, USA), anti-p-CHOP10 rabbit IgG (1:500), anti-CHOP10 rabbit IgG (1:300, cat. no. 15204-1-AP; ProteinTech Group, Inc.), anti-p-MEF2C rabbit IgG (1:500; cat. no. bs-5479R; BIOSS) and anti-MEF2C rabbit IgG (1:500; cat. no. 10056-1-AP; ProteinTech Group, Inc.) respectively. The secondary antibodies were HRP-conjugated goat anti-rabbit IgG (1:2,000) and goat anti-mouse IgG (1:2,000), which were diluted with skimmed milk (BD Biosciences). The abundance of the target protein was calculated relative to the abundance of the internal control protein, GAPDH, using Alphaview SA software (ProteinSimple).

Reverse transcription-quantitative polymerase chain reaction (RT-qPCR) analysis. The different groups of BMMSCs were added to 1 ml TRIzol to extract the total RNA and determine the RNA concentration and purity. An RT-PCR kit (Takara Bio, Inc., Osaka, Japan) was used to reverse transcribe the RNA into cDNA. Following dilution, the cDNA was treated with an amplification kit (Takara Bio, Inc.) for PCR, 2 μl cDNA was added to 20 μl of a PCR reaction system, following the manufacturer's protocol exactly to observe the SYBR-Green fluorescence signal. The primer sequences of the target genes are listed in Table I. The mRNA expression levels of HO-1 and CXCR3 were calculated as the relative quantity, using GAPDH as the reference. The relative expression of the target genes in each of the groups was calculated as the ratio of the relative level of the target gene to that of the GAPDH gene, using the Cq value as the statistical parameter (27). The primer sequences of the target genes are listed in Table I. The IEC-6 cells and the transplanted small bowel on day 7 post-transplantation were processed using the same steps as those described above. The relative mRNA expression levels of PCNA, ZO-1, MLK3, MKK3, P38, activating transcription factor 2 (ATF2), CHOP10 and MEF2C were also calculated using the relative quantity method (Table I).

Flow cytometry. The BMMSCs in each of the groups were trypsinized and adjusted to a density of $5x10^5$ cells/100 μl for further examination. The blank control tube of BMMSCs received no antibodies, whereas the other tubes received one of the three following antibody combinations: i) 0.625 μl anti-CD29-PE rat IgG (cat. no. 102207; BioLegend, Inc., San Diego, CA, USA) with 2.5 μl anti-CD34-FITC rat IgG (cat. no. sc-7324; Santa Cruz Biotechnology, Inc., Dallas, TX, USA) rat IgG; ii) 0.625 μl anti-CD45-PE rat IgG (cat. no. 202224) with 0.25 μl anti-CD90-FITC rat IgG (cat. no. 202503); or iii) 0.625 μl anti-RT1A-PE rat IgG (cat. no. 205208) with 0.25 μl anti-RT1B-FITC rat IgG (cat. no. 205305; all BioLegend, Inc.). The BMMSCs were incubated at 4˚C for 40 min, resuspended in PBS, centrifuged (300 x g for 5 min at 4˚C), fixed in 200 μl of 2% paraformaldehyde, and then analyzed by flow cytometry C6 (BD Biosciences). The lymphocytes in each of the groups were collected and adjusted to a density of $1x10^6$ cells/100 μl. Each sample received either 1.25 μl anti-CD3-APC rat IgG (cat. no. 17-0030) with 0.625 μl anti-CD25-PE rat IgG (cat. no. 12-0390; both eBioscience; Thermo Fisher Scientific, Inc.) or 1.25 μl anti-CD3-APC rat IgG with 0.625 μl anti-CD71-FITC rat IgG (cat. no. 204405; BioLegend, Inc.), and the lymphocytes were then incubated at 4˚C for 40 min, resuspended in PBS, centrifuged (500 x g for 5 min at 4˚C), fixed in 200 μl of 2% paraformaldehyde, and then analyzed by flow cytometry C6 (BD Biosciences).

ELISA. The supernatants from each of the groups of cells were collected following centrifugation and stored at -80˚C. Interleukin (IL)-2 and IFN-γ kits (R&D Systems, Inc. Minneapolis, MN, USA) were used to assess the concentrations of cytokines, in accordance with the manufacturer's protocol.

Animal model. The small bowel transplantation donors were healthy male Brown Norway rats (aged 6-8 weeks, weighing 180-200 g, n=40), and the recipients for small bowel transplantation were healthy male Lewis rats (aged 6-8 weeks, weighing 180-200 g, n=70). All animals were provided by the Experimental Animal Center of the Academy of Military Medical Sciences and standard rat food was provided *ad libitum*. The experimental animals were kept at 23˚C with 50% humidity and a 12 h light/dark cycle for 2 weeks, with free access to water and food, and regular replacement of bedding prior to the experiments. All experiments on animals followed the experimental animal ethical regulations, and were approved by the Ethics Committee of Tianjin First Central Hospital. The small bowel transplantation model used was established using the method described by Yin *et al* (18). The rats were divided into six groups: i) NSBT group, sham-operated without small bowel transplantation; ii) IsoT group, received an isogeneic transplantation of the small bowel from genetically identical hosts (Lewis); iii) NS group, injected intravenously with 1 ml sterile normal saline (NS; 0.9% sodium chloride solution) from the dorsal penile vein; iv) MSCs group, injected with a single-cell suspension including $5x10^6$ BMMSCs; v) Ad-HO/MSCs group, injected with a single-cell suspension including $5x10^6$ Ad-HO-1/MSCs; and vi) Ad-(CXCR3 + HO)/MSCs group, injected with a single-cell suspension of $5x10^6$ Ad-(CXCR3 + HO-1)/MSCs. On day 7 post-small bowel transplantation, samples from each of the groups were acquired and analyzed.

Statistical analysis. SPSS statistical software, version 17.0 (SPSS, Inc., Chicago, IL, USA) was used for all statistical analysis. Normally distributed data are presented as the mean ± standard deviation. The significance of differences between groups were assessed using Student's t-test (single comparisons) or one-way analysis of variance with Least Significant Difference and Student-Newman-Keuls post hoc comparison. $P<0.05$ was considered to indicate a statistically significant difference. GraphPad Prism 5.0 software (GraphPad Software, Inc., La Jolla, CA, USA) was used to plot data for presentation.

Table I. Primer sequences for reverse transcription-quantitative polymerase chain reaction analysis.

Gene	Forward (5'-3')	Reverse (5'-3')
HO-1	CTGGCTCTTTTCTTGG	ATGGTCAGAACATGGAC
CXCR3	TCATGGCCTACTGCTATGC	CGACTTGGCCACGTCTAC
GAPDH	CCGTATCGGACGCCTGGTTAC	GCCGTGGGTAGAGTCATACTGGAAC
MLK3	TCCCAGACTCAGATCCCTTCTG	CCAGTGTATGCTATGCCTCCTC
MKK3	CACCCGTTCTTCACCTTGCAC	ACTTGGGACAGCTAGTTGCGAG
P38	CCCAGCAGTCCTATCCACG	TCTCCCTTTGTTCGGTTTGC
ATF2	TGAGTTGGCAAGTCCATTCG	GCTATCCTGGTGAGTTGTTTCTAC
CHOP10	CTTGCTGAAGAGAACGAG	CATGTGCACTGGAGATTAC
MEF2C	GGGTCACCGTAGGCATAGAG	CGACAAAGTCCAGCTTATGC
PCNA	AACTTGGAATCCCAGAACAGG	CTGTAGGAGACAGTGGAGTGGC
ZO-1	TGAGCCTTGAACTTTGACCTC	GAAATCGTGCTGATGTGCC

HO-1, heme oxygenase-1; CXCR3, CXC-chemokine receptor CXCR3; MLK3, mixed lineage kinases 3; MKK3, mitogen-activated protein kinase kinase 3; ATF2, activating transcription factor 2; CHOP10, C/EBP homologous protein-10; MEF2C, myocyte enhancer factor type 2C; PCNA, proliferating cell nuclear antigen; ZO-1, zonula occludens-1.

Results

Verification of BMMSCs transfected with Ad, HO-1, CXCR3, and CXCR3 + HO-1. In terms of morphological aspects, the third generation BMMSCs typically exhibited a spindle shape and it was not possible to differentiate them into adipocytes and osteoblasts. The positivity of the expression of the extracellular markers CD29, CD90 and RT1A on BMMSCs was >95% (18). The morphological changes of the Ad/MSCs, Ad-HO/MSCs, Ad-CXCR3/MSCs and Ad-(HO + CXCR3)/MSCs were not marked different compared with those of BMMSCs (untreated control), and the cells remained spindle-shaped (Fig. 1A).

For the identification of gene expression, low positive expression of the HO-1 and CXCR3 proteins was observed in the BMMSCs and Ad/MSCs. The protein expression of HO-1 was high and that of CXCR3 protein was low in the Ad-HO MSCs (Fig. 1B). The protein expression of CXCR3 was high and that of HO-1 was low in the Ad-CXCR3/MSCs (Fig. 1C). The protein expression of HO-1 and CXCR3 were high in the Ad-(HO + CXCR3)/MSCs (Fig. 1D).

Phenotypically, the positive expression of CD29, CD90 and RT1A on the BMMSCs exposed to different treatments were >95%, with no significant difference between the five groups (Fig. 1E). The negative expression of CD34, CD45 and RT1B exposed to different treatments were >95%, with no significant difference between the five groups (Fig. 1E).

The viability of the BMMSCs transduced with the different genes was similar to that of the normal BMMSC (Fig. S1A-F). The protein and mRNA concentrations of HO-1 in the Ad-HO/MSCs and Ad-(HO + CXCR3)/MSCs were significantly higher than those in the BMMSCs, Ad/MSCs and Ad-CXCR3/MSCs ($P<0.05$; Fig. S1G). The protein and mRNA concentrations of CXCR3 in the Ad-CXCR3/MSCs and Ad-(HO + CXCR3)/MSCs were significantly higher than those in the BMMSCs, Ad/MSCs and Ad-HO/MSCs ($P<0.05$; Fig. S1H). These results suggest that the CXCR3, HO-1 and HO-1 + CXCR3 genes were successfully transfected into BMMSCs, did not affect the morphology of the BMMSCs and exhibited no toxic effects.

Establishment of the TNF-α/IEC-6 model, IEC-6 cell viability and BMMSC chemotaxis. The protein and mRNA levels of the tight junction protein, ZO-1, in the injured intestinal epithelium model (TNF-α/IEC-6, referred to as the Model group) were significantly lower than those in the normal IEC-6 cells ($P<0.05$; Fig. 2A). This suggests that the model of IEC-6 injury was successfully established, as indicated by the presence of damaged intestinal epithelial cells.

IEC-6 viability in the Model and L groups was similar and significantly lower than that in the Normal group ($P<0.05$). The viability of IEC-6 in the S + L, MSCs + L, Ad/MSCs + L, and Ad-HO/MSCs + L groups were similar, which were lower than the that in the Normal group ($P<0.05$) and significantly higher than that in the Model and L groups ($P<0.05$). IEC-6 viability in the Ad-CXCR3/MSCs + L and Ad-(CXCR3 + HO)/MSCs + L groups were similar ($P<0.05$), which was lower than that in the Normal group and significantly higher than that in all other groups ($P<0.05$; Fig. 2B). These results suggest that BMMSCs improved the viability of injured IEC-6 cells. The effects of the HO-1 gene-modified Ad-HO-1/BMMSCs on IEC-6 cells was similar to that of the BMMSCs, whereas the effects of the CXCR3 gene-modified Ad-CXCR3/BMMSCs and Ad-(HO-1 + CXCR3)/BMMSCs were more substantial.

Following co-culture for 24 h, the numbers of migrated BMMSCs (Fig. 2C) in the Ad-CXCR3/MSCs + L and Ad-(CXCR3 + HO)/MSCs + L groups were significantly higher than the numbers in the L, MSCs + L, Ad/MSCs + L and Ad-HO/MSCs + L groups (Fig. 2Da-f), $P<0.05$). Only lymphocytes migrated in the L group and lymphocytes appear as blue dots (Fig. 2Da). There was no significant difference in the number of migrated BMMSCs between the MSCs + L, Ad/MSCs + L and Ad-HO/MSCs + L groups, and the BMMSCs had a polygonal shape (Fig. 2D). A large number of BMMSCs migrated at 1 h in the Ad-CXCR3/MSCs + L and Ad-(CXCR3 + HO)/MSCs + L (Fig. 2E) groups, and gradually increased over time. Few BMMSCs had migrated at 1 h in the Ad/MSCs + L and Ad-HO/MSCs + L groups, and a small number of BMMSCs began to migrate at 4 h (Fig. 2F).

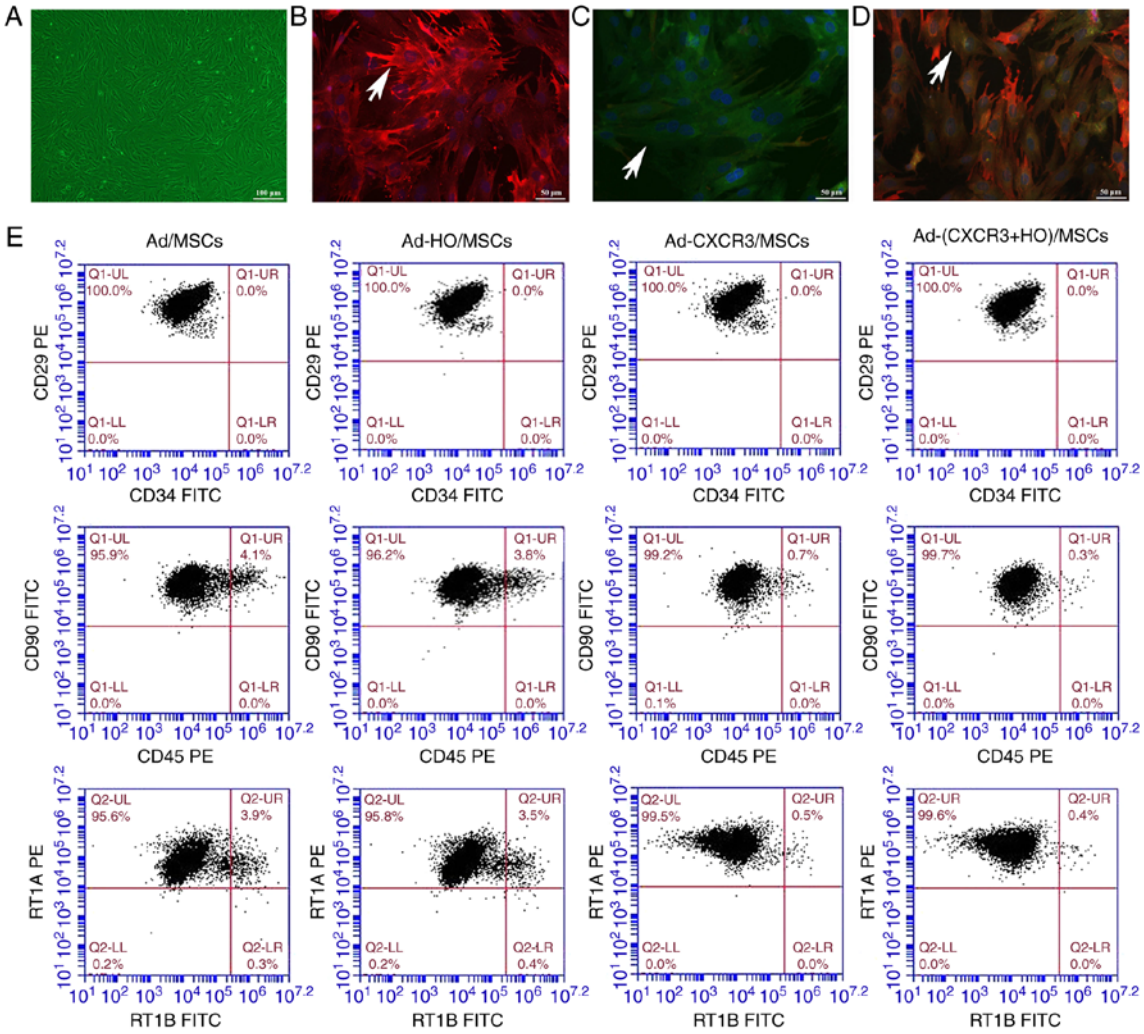

Figure 1. Morphology, phenotype, gene expression and viability of the different groups of BMMSCs. (A) Cellular morphology of Ad-MSCs (scale bar, 100 μm). The red fluorescence indicates HO-1 protein, the green fluorescence indicates CXCR3 protein and the blue fluorescence indicates the nucleus. (B) Positive expression of HO-1 protein was high in Ad-HO/MSCs (indicated by white arrows), (C) Positive expression of CXCR3 protein was high in Ad-CXCR3/MSCs (indicated by white arrows); scale bar, 50 μm. (D) Positive expression of both HO-1 and CXCR3 proteins was high in Ad-(CXCR3 + HO)/MSCs (indicated by white arrows); scale bar, 50 μm. (E) Changes in cell surface markers of BMMSCs transfected with different genes. BMMSCs, bone marrow mesenchymal stem cells; Ad, adenovirus; CXCR3, CXC-chemokine receptor CXCR3; HO-1, heme oxygenase-1.

These results indicate that the CXCR3 gene was capable of increasing the chemotactic ability of BMMSCs, allowing the rapid migration of a large number of cells through the Transwell membrane, which were able to reach the damaged IEC-6 cells where they mediated their effector function.

Effect of BMMSCs on tight junction proteins and the apoptosis of damaged IEC-6 cells. The positive expression of ZO-1 (assessed via green fluorescence in Fig. 3Aa-j) was significant in the Normal group. The positive expression of ZO-1 decreased significantly in the Model group, and the intercellular tight junctions were severely damaged. The positive expression of ZO-1 also decreased significantly in the L group, exhibiting destruction similar to that in the Model group. The positive expression of ZO-1 increased significantly in the S + L, MSCs + L, Ad-MSCs + L and Ad-HO/MSCs + L groups, with similar results observed in these four groups. The positive expression of ZO-1 increased the most markedly in the Ad-CXCR3/MSCs + L and Ad-(CXCR3 + HO)/MSCs + L groups (Fig. 3A). The concentrations of ZO-1 protein in the Model and L groups did not differ significantly, and both were significantly lower than that in the Normal group ($P<0.05$). The protein concentrations of ZO-1 in the S + L, MSCs + L, Ad/MSCs + L and Ad-HO/MSCs + L groups were higher than those in the Model and L groups ($P<0.05$), and all were lower than that in the Normal group ($P<0.05$). There were no statistically significant differences among the S + L, MSCs + L, Ad/MSCs + L and Ad-HO/MSCs + L groups. The Ad-CXCR3/MSCs + L and Ad-(CXCR3 + HO)/MSCs + L groups exhibited a similar protein concentration of ZO-1, which was lower than that in the Normal group ($P<0.05$), and significantly higher than that in all other groups ($P<0.05$; Fig. 3Aa-j).

No apoptosis of IEC-6 cells was detected in the Normal group, however, levels of apoptosis in the Model and L groups were increased significantly, and were higher than apoptosis in the S + L, MSCs + L, Ad/MSCs + L and Ad-HO/MSCs + L groups ($P<0.05$). However, no significant differences were observed among these four groups. The levels of IEC-6 apoptosis in the Ad-CXCR3/MSCs + L and Ad-(CXCR3 + HO)/MSCs + L groups did not differ significantly ($P=0.471$), but they were

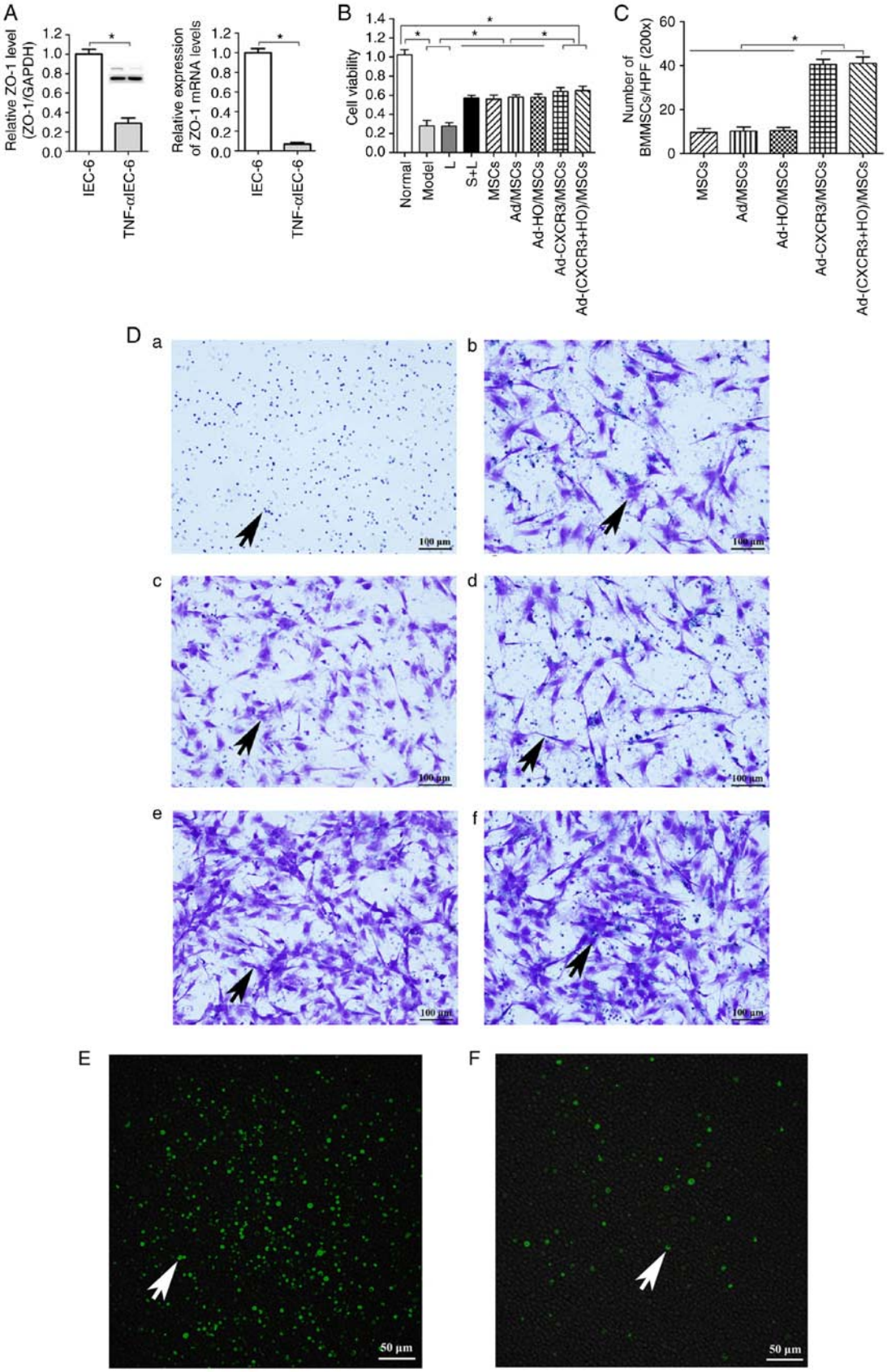

Figure 2. Validation of the TNF-α/IEC-6 model, IEC-6 cell viability and BMMSC chemotaxis. (A) Protein and mRNA content of ZO-1 in IEC-6 cells and TNF-α/IEC-6. (B) IEC-6 viability in each of the groups was detected. (C) BMMSC migration; the number of migrated BMMSCs in the Ad-CXCR3/MSCs + L and Ad-(CXCR3 + HO)/MSCs + L groups were all higher than in the other groups. (D) Migrated BMMSCs across Transwell membranes (indicated by black arrows): (a) L group, (b) MSC + L group, (c) Ad/MSCs + L group, (d) Ad-HO/MSCs + L group, (e) Ad-CXCR3/MSCs + L group, and (f) Ad-(CXCR3 + HO)/MSCs + L (scale bar, 100 μm). (E) A large number of CXCR3-modified BMMSCs migrated together at 1 h, whereas a (F) small number of BMMSCs without the CXCR3 gene modified began to migrate at 4 h (indicated by white arrows; scale bar, 50 μm). *P<0.05. IEC-6, intestinal epithelial crypt cell line-6; ZO-1, zonula occludens-1; TNF-α; tumor necrosis factor-α; BMMSCs, bone marrow mesenchymal stem cells; Ad, adenovirus; CXCR3, CXC-chemokine receptor CXCR3; HO-1, heme oxygenase-1; L, lymphocytes; S, S203580.

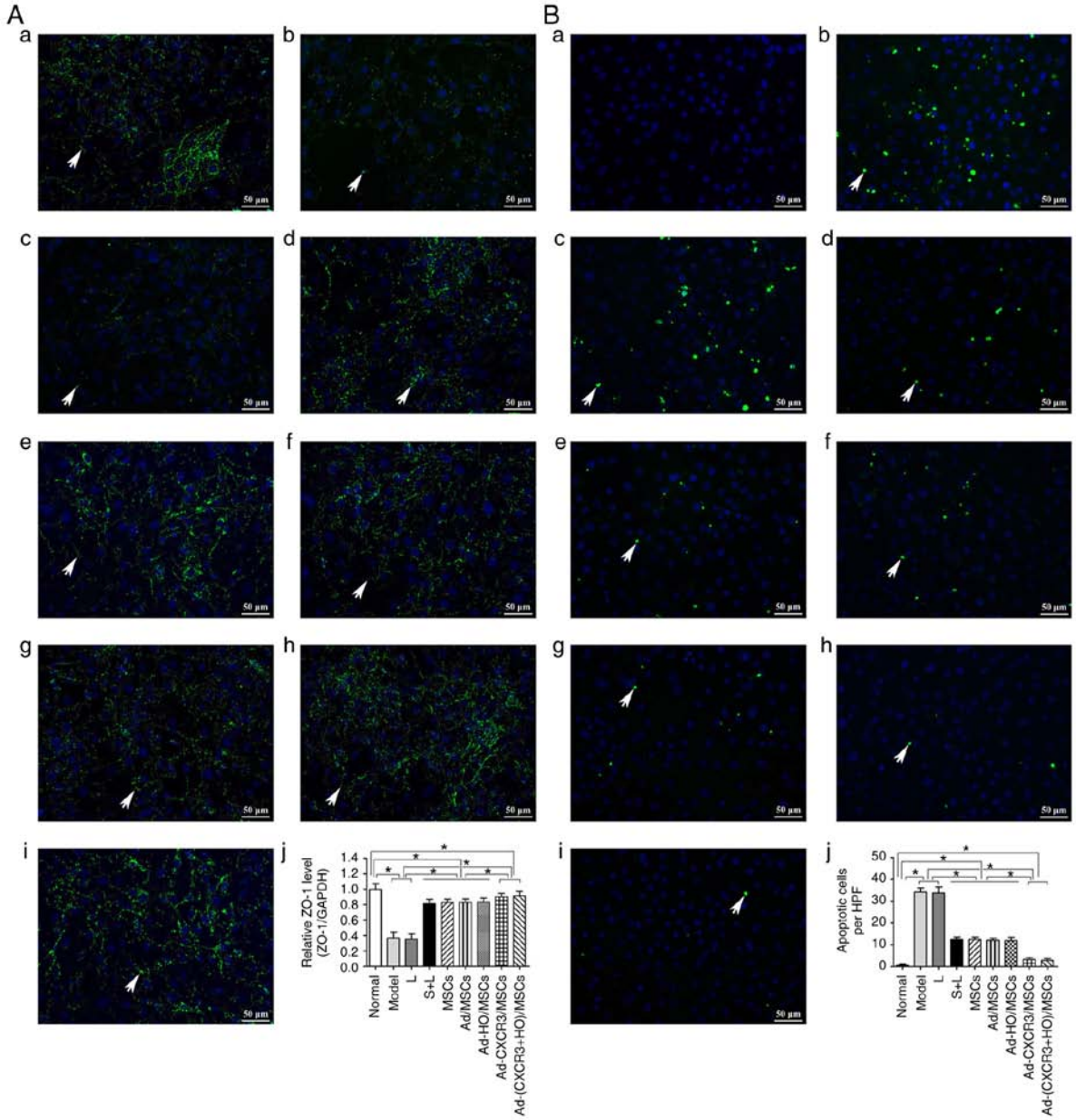

Figure 3. Expression of tight junction protein, ZO-1, and IEC6 apoptosis. (A) Expression of ZO-1 in each group, with the cell nucleus shown in blue and tight junction protein, ZO-1 (indicated by white arrows) shown in green. (a) Normal, (b) Model, (c) L, (d) S + L, (e) MSCs + L, (f) Ad/MSCs + L, (g) Ad-HO/MSCs + L, (h) Ad-CXCR3/MSCs + L and (i) Ad-(CXCR3 + HO)/MSCs + L groups (scale bar, 50 μm); (j) protein expression of ZO-1 in each group. (B) Apoptosis of IEC-6 cells in each of groups, with the cell nucleus shown in blue and apoptotic bodies (indicated by white arrows) shown in green. (a) Normal, (b) Model, (c) L, (d) S + L, (e) MSCs + L, (f) Ad/MSCs + L, (g) Ad-HO/MSCs + L, (h) Ad-CXCR3/MSCs + L, and (i) Ad-(CXCR3 + HO)/MSCs + L groups (scale bar, 50 μm); (j) apoptosis of IEC-6 cells. *P<0.05. IEC-6, intestinal epithelial crypt cell line-6; ZO-1, zonula occludens-1; MSCs, bone marrow mesenchymal stem cells; Ad, adenovirus; CXCR3, CXC-chemokine receptor CXCR3; HO-1, heme oxygenase-1; L, lymphocytes; S, S203580.

significantly lower than that in all other groups, with the exception of the Normal group (P<0.05; Fig. 3Ba-j).

These results suggest that the expression of the intestinal tight junction protein, ZO-1, decreased and apoptosis increased when the IEC-6 cells were damaged. In addition, the BMMSCs increased the expression of ZO-1 and decreased apoptosis of the damaged IEC6 cells. The effects of the Ad-HO/MSCs were similar to those of the BMMSCs, and the effects of the Ad-CXCR3/MSCs and Ad-(CXCR3 + HO)/MSCs were more marked than those of the Ad-HO/MSCs and BMMSCs.

Lymphocyte activity in each treatment group. The proportions of $CD3^+$ $CD25^+$ and $CD3^+$ $CD71^+$ within the $CD3^+$ lymphocyte population were relatively low in the normal rat lymphocytes. The proportions of $CD3^+$ $CD25^+$ and $CD3^+$ $CD71^+$ cells in the L group were significantly higher than those of the other groups (P<0.05). The proportions of $CD3^+CD25^+$ cells and $CD3^+CD71^+$ cells in the Ad-CXCR3/MSCs + L and Ad-(CXCR3 + HO)/MSCs + L groups were similar to those in the normal rat lymphocytes (P>0.05), but significantly lower than those in the MSCs + L, Ad-MSCs + L and Ad-HO/MSCs + L groups (P<0.05; Fig. 4A-J). Increased concentrations of IL-2 and IFN-γ indicate enhanced lymphocyte activity, and vice versa. The concentrations of IL-2 and IFN-γ in the L group were significantly higher than those in the other groups (P<0.05). The concentrations of IL-2 and IFN-γ were

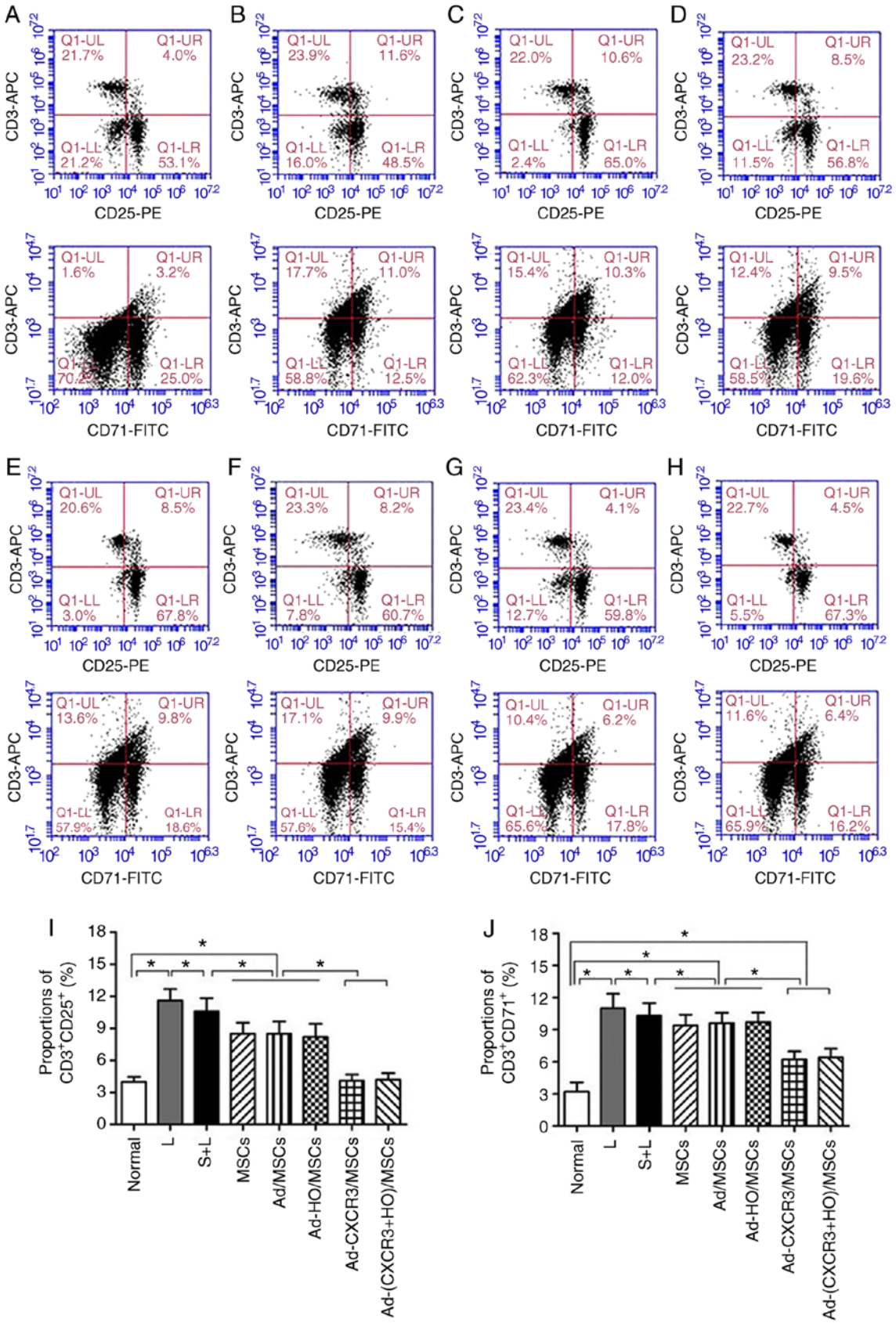

Figure 4. Proportions of $CD3^+CD25^+$ and $CD3^+CD71^+$, and supernatant concentrations of IL-2 and IFN-γ in the different groups of T lymphocytes. Proportions of $CD3^+$ $CD25^+$ and $CD3^+$ $CD71^+$ in (A) normal rat lymphocytes, and the (B) L, (C) S + L, (D) MSCs + L, (E) Ad/MSCs + L, (F) Ad-HO/MSCs + L, (G) Ad-CXCR3/MSCs + L and (H) Ad-(CXCR3 + HO)/MSCs + L groups. The proportions of $CD3^+$ $CD25^+$ and $CD3^+$ $CD71^+$ within the $CD3^+$ lymphocyte population were relatively low in the normal rat lymphocytes (4.0 and 3.2%, respectively). Expression was high (11.6 and 11.0%) in the L group, and in the S + L group (10.6% and 10.3%). Expression was significantly lower in the MSCs + L, Ad/MSCs + L and Ad-HO/MSCs + L groups compared with that in the L group ($P<0.05$). (I) The proportions of $CD3^+CD25^+$ cells in the Ad-CXCR3/MSCs + L and Ad-(CXCR3 + HO)/MSCs + L group were 4.1 and 4.5%, respectively, and those of (J) $CD3^+CD71^+$ cells were 6.2 and 6.4%, respectively, which were similar to those in normal lymphocytes ($P>0.05$, but were significantly lower compared with those in other groups ($P<0.05$).

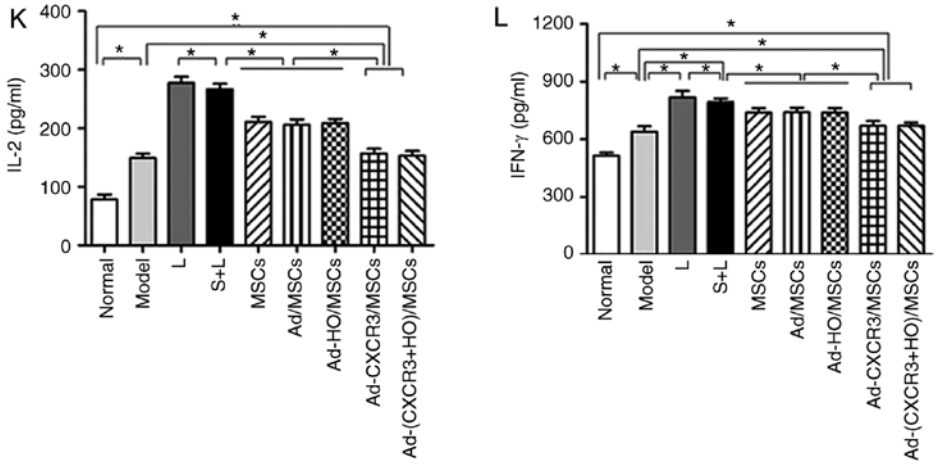

Figure 4. Continued. Concentrations of (K) IL-2 and (L) IFN-γ were relatively low in the normal group, significantly higher in the model group (P<0.05), and similar in the Ad-CXCR3/MSCs + L and Ad-(CXCR3 + HO)/MSCs + L groups, which were higher than those in the Normal group (P<0.05), but significantly lower than in the other groups (P<0.05). *P<0.05. MSCs, bone marrow mesenchymal stem cells; Ad, adenovirus; CXCR3, CXC-chemokine receptor CXCR3; HO-1, heme oxygenase-1; L, lymphocytes; S, S203580; IL-2, interleukin-2; IFN-γ, interferon-γ.

decreased and at similar levels in the MSCs + L, Ad-MSCs + L and Ad-HO/MSCs + L groups, which were higher than those in the Normal and Model groups (P<0.05). The concentrations of IL-2 and IFN-γ in the Ad-CXCR3/MSCs + L and Ad-(CXCR3 + HO)/MSCs + L groups were decreased significantly and were lower than those observed in the other groups (P<0.05; Fig. 4K and L).

These results indicate that BMMSCs inhibited the activation of lymphocytes, and the effects of the Ad-HO/MSCs were similar to those of BMMSCs. The inhibitory effects of the CXCR3 gene-modified BMMSCs were more marked, which may be attributed to the ability of Ad-CXCR3/MSCs and Ad-(CXCR3 + HO)/MSCs to compete with preliminary activated T lymphocytes for CXCR3 ligands. This results in the inability of T lymphocytes to bind with these ligands, inhibiting further T lymphocyte activation, and decreasing the secretion of inflammatory cytokines.

P38-MAPK pathway-related protein and mRNA changes in the IEC-6 cells of the treatment groups. The present study subsequently analyzed the p38-MAPK upstream phosphorylated proteins, p-MLK3, p-MKK3 and p-p38, and downstream phosphorylated proteins p-ATF2, p-CHOP10 and p-MEF2C in the MAPK pathway, and PCNA protein of the target cells. The protein and mRNA expression levels of p-MLK3 and p-MKK3 were high in all experimental groups, with the exception of the Normal group; however, there was no difference among these groups (Fig. 5A and B). These results suggest that the upstream proteins in the p38-MAPK pathway are not involved in the repair of damaged IEC-6 cells by the genetically modified BMMSCs.

The protein and mRNA expression levels of p-p38, p-ATF2, p-CHOP10 and p-MEF2C were high in the Model and L groups, and these levels were higher than those in all other groups (P<0.05). Following use of the p38 MAPK inhibitor, S203580 (S + L group), the expression levels of p-p38 and associated downstream molecules were significantly decreased to levels lower than those in the Model and L groups (P<0.05) (Figs. 5C and 6A-E). The protein and mRNA expression levels of p-p38, p-ATF2, p-CHOP10 and p-MEF2C in the Ad-CXCR3/MSCs + L and Ad-(CXCR3 + HO)/MSCs + L groups decreased, and were significantly lower than all other experimental groups (P<0.05); however, there was no significant difference between these two groups. The results of the S + L, MSCs + L, Ad-MSCs + L, and Ad-HO/MSCs + L groups exhibited no statistically significant difference (Fig. 5C and 6A-E). The protein, p-CHOP10, was histochemically stained (Fig. 6F). The positive expression of p-CHOP10 in the Model and L groups was significantly higher than that in the other groups (P<0.05). The S + L, MSCs + L, Ad/MSCs + L and Ad-HO/MSCs + L groups exhibited similar positive expression of p-CHOP10, the level of which was higher than that in the Ad-CXCR3/MSCs + L and Ad-(CXCR3 + HO)/MSCs + L groups (P<0.05); the latter two groups were not significantly different (P=0.242; Fig. 6F). These results indicate that, as an inhibitor of p38 protein phosphorylation, S203580 inhibits the activation of the p38-MAPK pathway, thereby significantly inhibiting the function of downstream protein expression without significantly altering the expression of the upstream protein in the pathway. As BMMSCs exhibited effects similar to that of S203580, it was hypothesized that they exert a reparative effect on damaged IEC-6 cells through the p38 MAPK pathway. The effects of the HO-1 gene-modified BMMSCs were similar to those of BMMSCs, suggesting that HO-1 provided no advantage. In addition, the CXCR3-modified BMMSCs demonstrated more marked effects the BMMSCs, indicating that the CXCR3 gene synergistically enhanced the reparative capacity of the BMMSCs.

The protein and mRNA expression levels of PCNA in the IEC-6 cells of the Normal group were higher than those in the Model and L groups (P<0.05); the expression levels in these latter two groups were lower than in all the other experimental groups (P<0.05). The protein and mRNA expression levels of PCNA in the IEC-6 cells of the MSCs + L, Ad/MSCs + L and Ad-HO/MSCs + L groups were similar, which were higher than that in the S + L group. The Ad-CXCR3/MSCs + L

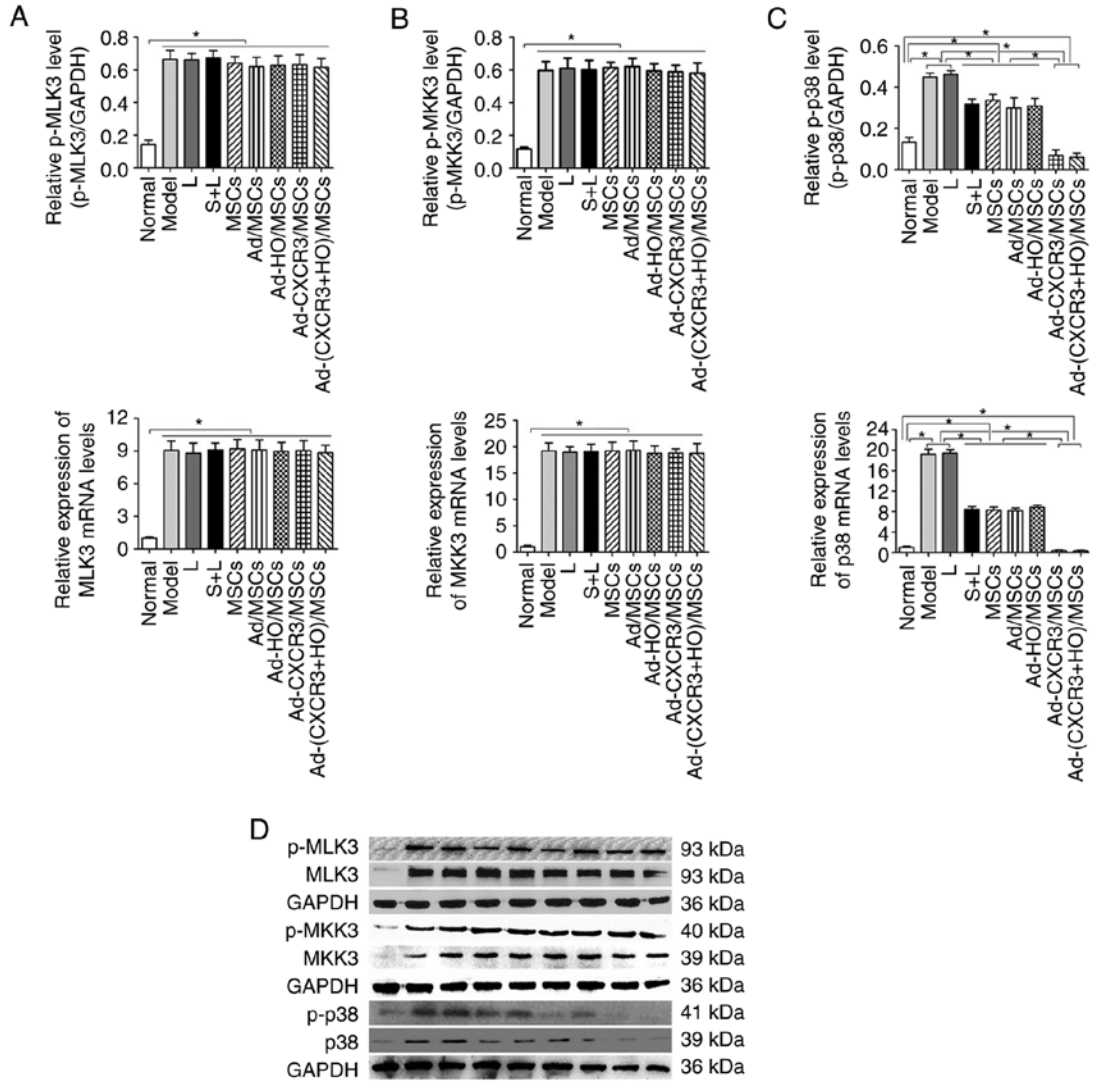

Figure 5. Relative expression levels of p-MLK3, MLK3, p-MKK3, MKK3, p-p38 and p38 in each of the treatment groups. The protein and mRNA expression levels of (A) MLK3 and (B) MKK3 were high in all experimental groups, with the exception of the Normal group, and the levels of p-MKK3 and p-MLK3 were significantly higher than that in the Normal group (P<0.05). (C) Protein and mRNA expression levels of p38 were highest in the Model and L groups, which were significantly higher than in all other groups (P<0.05). The expression levels of p38 and p-p38 in the Ad-CXCR3/MSCs + L and Ad-(CXCR3 + HO)/MSCs + L groups were the lowest, which were significantly lower than those of the other experimental groups (P<0.05). *P<0.05. (D) Expression of p-MLK3, MLK3, p-MKK3, MKK3, p-p38 and p38 in each of the treatment groups as demonstrated by western blotting. MSCs, bone marrow mesenchymal stem cells; Ad, adenovirus; CXCR3, CXC-chemokine receptor CXCR3; HO-1, heme oxygenase-1; L, lymphocytes; S, S203580; MLK3, mixed lineage kinases 3; MKK3, mitogen-activated protein kinase kinase 3; p-, phosphorylated.

and Ad-(CXCR3 + HO)/MSCs + L groups exhibited similar results, exhibiting higher expression than in the other groups (P<0.05; Fig. 6E). These results suggest that, as a downstream target protein in the p38-MAPK pathway, the expression of PCNA was influenced by p38-MAPK signaling. The effects of the HO-1 gene-modified BMMSCs were similar to those of BMMSCs, indicating that HO-1 provided no advantage. In addition, the CXCR3-modified BMMSCs exhibited more marked effects than the BMMSCs.

Expression of p38-MAPK-related proteins in a rejection model of small bowel transplantation. The protective effects of the Ad-(CXCR3 + HO)/MSCs and Ad-HO/MSCs groups on the damaged IEC-6 cells were the most marked on post-operative day 7 in the rejection model of small bowel transplantation. Therefore, p38-MAPK-related proteins were detected in the transplanted intestinal tissues of rats on day 7 post-transplantation. The results showed that the upstream proteins p-MLK3, p-MKK3 and p-p38, and downstream proteins p-ATF2, p-CHOP10 and p-MEF2C of the p38-MAPK pathway, and the target protein, PCNA, exhibited low expression in the Normal and IsoT groups, which were significantly different from all other groups (P<0.05; Fig. 7A-I). p-MLK3 and p-MKK3 were expressed at high levels in the NS, MSCs, Ad-HO/MSCs, and Ad-(CXCR3 + HO)/MSCs groups (Fig. 7A and B). The expression of p-p38 was significantly different among the groups as follows: Expression in the Ad-(CXCR3 + HO)/MSCs group was significantly lower than that in all other experimental groups (P<0.05); expression in the Ad-HO/MSCs group was lower than that in the MSCs and NS (P<0.05) groups; and expression in the MSCs group was lower than that in the NS group (P<0.05; Fig. 7C). The expression levels of p-ATF2, p-CHOP10 and p-MEF2C in the Ad-(CXCR3 + HO)/MSCs were significantly lower than those in the Ad-HO/MSCs

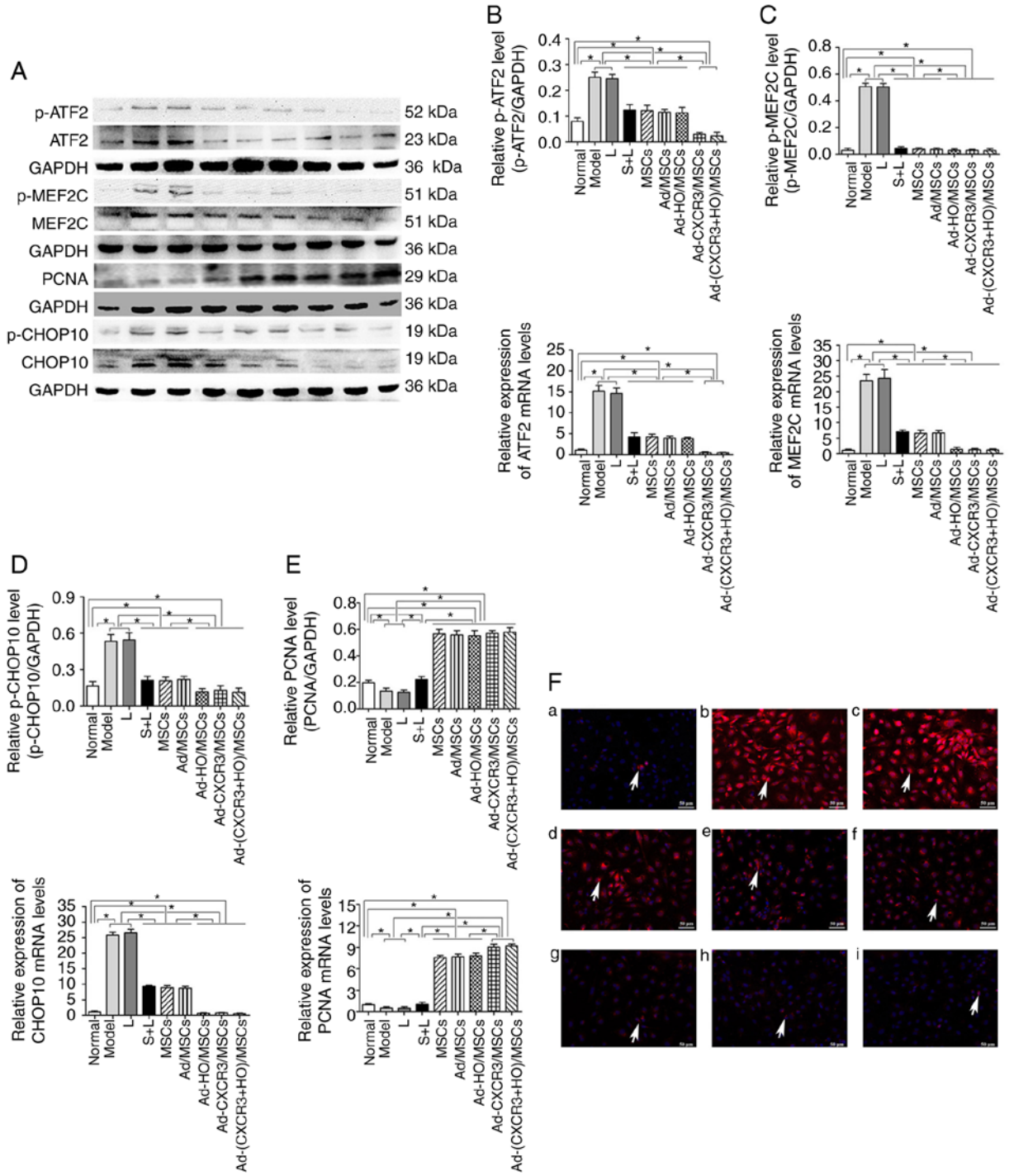

Figure 6. Relative expression of p-ATF2, ATF2, p-MEF2C, MEF2C, PCNA, p-CHOP10 and CHOP10, and p-CHOP10 positivity in each treatment group. (A) Expression of p-ATF2, ATF2, p-MEF2C, MEF2C, PCNA, p-CHOP10 and CHOP10 in each treatment group as demonstrated by western blotting. Protein and mRNA expression of (B) ATF2 to p-ATF2, (C) MEF2C to p-MEF2C, (D) PCNA and (E) CHOP10 to p-CHOP10 in each group. (F) p-CHOP10 (indicated by white arrows) exhibited low positive rate in the (a) Normal group but was expressed at high levels when the IEC-6 cells were damaged: (b) Model and (c) L groups. Compared with the (d) S + L, (e) MSCs + L, and (f) Ad-MSCs + L groups, p-CHOP10-positivity was significant lower in the (g) Ad-HO/MSCs + L, (h) Ad-CXCR3/MSCs + L and (i) Ad-(CXCR3 + HO)/MSCs + L groups. Scale bar, 50 μm. *P<0.05. MSCs, bone marrow mesenchymal stem cells; Ad, adenovirus; CXCR3, CXC-chemokine receptor CXCR3; HO-1, heme oxygenase-1; L, lymphocytes; S, S203580; ATF2, activating transcription factor 2; MEF2C, myocyte enhancer factor type 2C; PCNA, proliferating cell nuclear antigen; CHOP10, C/EBP homologous protein-10; p-, phosphorylated.

(P<0.05), whereas levels in the Ad-HO/MSCs were lower than those in the MSCs (P<0.05), and levels in the NS group were the highest (Fig. 7D-F). The expression of PCNA was significantly higher in the Ad-(CXCR3 + HO)/MSCs group compared with that in the other experimental groups (P<0.05). The expression of PCNA in the Ad-HO/MSCs group was higher than that in the MSCs and NS groups (P<0.05). The MSCs group exhibited higher expression of PCNA than the NS group (P<0.05) (Fig. 7G). The expression of ZO-1 was significantly higher in the NBST and IsoT groups compared with that in the other experimental groups. In the Ad-(CXCR3 + HO)/MSCs group was higher than that in the Ad-HO/MSCs, MSCs and NS groups (P<0.05). In the

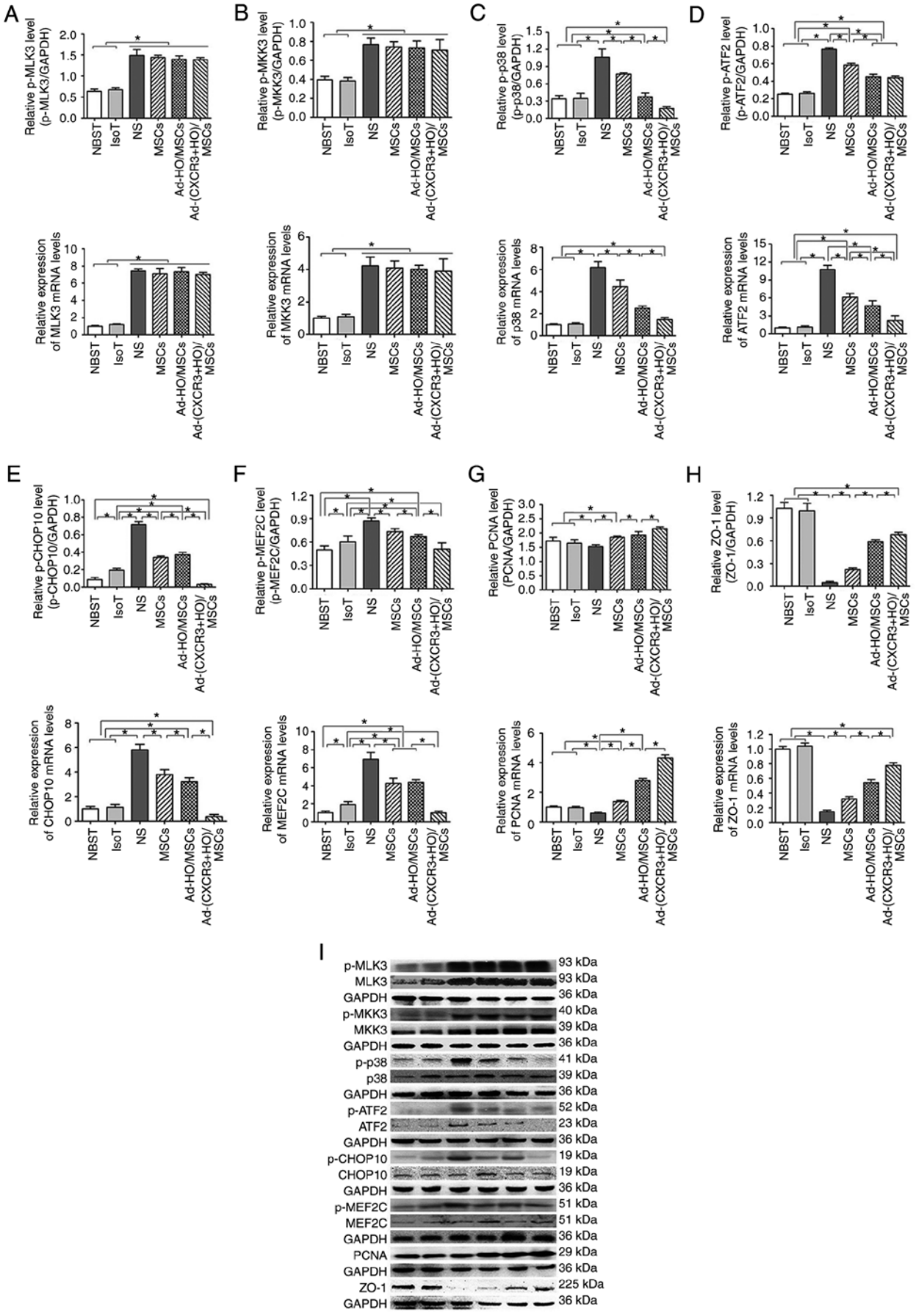

Figure 7. p38-MAPK pathway-related protein and mRNA expression, and immunohistochemical expression of p-CHOP10 on day 7 post-small bowel transplantation. Protein and mRNA expression of (A) MLK3 to p-MLK3, (B) MKK3 to p-MKK3, (C) p38 to p-p38, (D) ATF2 to p-ATF2, (E) CHOP10 to p-CHOP10, (F) MEF2C to p-MEF2C, (G) PCNA and (H) ZO-1 in each group. (I) Expression of related protein of the p38-MAPK pathway as demonstrated by western blotting. *P<0.05..

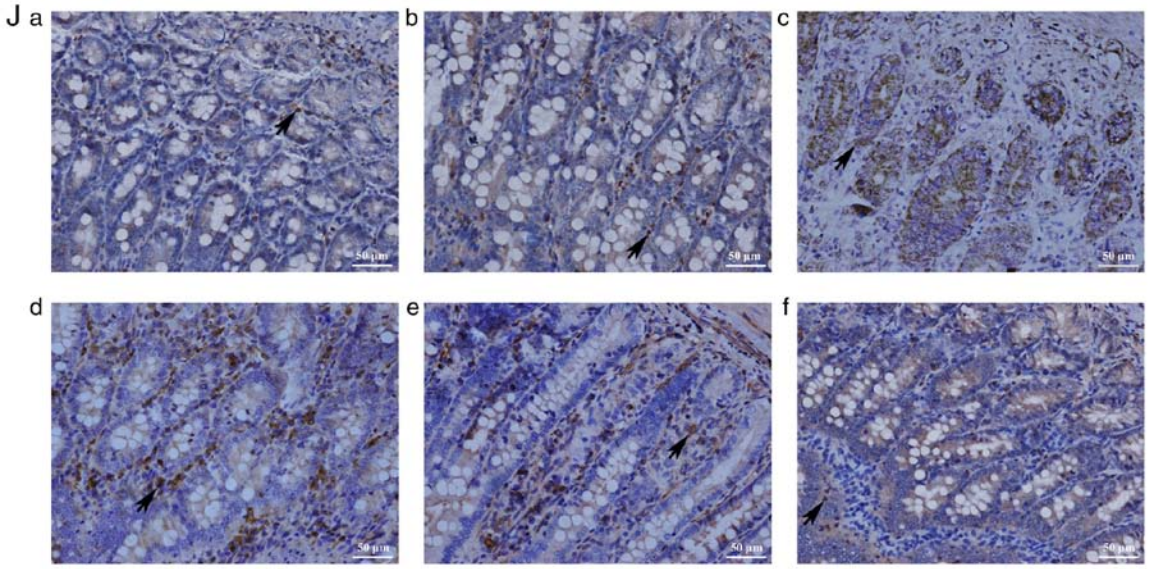

Figure 7. Continued. (J) Immunohistochemical expression of p-CHOP10 on day 7 post-small bowel transplantation: (a) NBST, (b) IsoT, (c) NS, (d) MSCs, (e) Ad-HO/MSCs and (f) Ad-(CXCR3 + HO)/MSCs groups. Expression was significantly lower in the Normal group than in the other groups, with the exception of the Ad-(CXCR3 + HO)/MSCs group ($P<0.05$); expression in the IsoT group was lower than that in the NS, MSCs and Ad-HO/MSCs groups ($P<0.05$). Expression in the Ad-HO/MSCs group was lower than that in the MSCs and NS groups ($P<0.05$). Expression in the NS group was the highest, and expression in the Ad-(CXCR3 + HO)/MSCs group was significantly lower than that in all experimental groups. MSCs, bone marrow mesenchymal stem cells; Ad, adenovirus; CXCR3, CXC-chemokine receptor CXCR3; HO-1, heme oxygenase-1; L, lymphocytes; S, S203580; IsoT, isogeneic transplantation of the small bowel from genetically identical host; NS, injected intravenously with normal saline (0.9% sodium chloride solution) CHOP10, CHOP10, C/EBP homologous protein-10; MLK3, mixed lineage kinases 3; MKK3, mitogen-activated protein kinase kinase 3; ATF2, activating transcription factor 2; MEF2C, myocyte enhancer factor type 2C; PCNA, proliferating cell nuclear antigen; p-, phosphorylated.

Ad-HO/MSCs was higher than that in the MSCs and NS groups ($P<0.05$). The expression of ZO-1 in the NS groups was the lowest. (Fig. 7H). The results of the above proteins detected by western blot are summarized in Fig. 7I. The positive expression of p-CHOP10 in the Ad-(CXCR3 + HO)/MSCs group was significantly lower than that in the other groups (Fig. 7J). These results suggest that BMMSCs may repair the damaged intestinal epithelial cells via the p38-MAPK pathway. The HO-1 gene-modified BMMSCs showed more marked protective effects than the BMMSCs; however, the effects of BMMSCs co-modified with the CXCR3 and HO-1 genes were the most marked.

Discussion

Stem cells are pluripotent cells with the ability to self-replicate. BMMSCs are one of the most representative types of stem cells. BMMSCs have the properties of proliferation, differentiation, and immune-modulation *in vitro*, and can promote tissue repair in damaged tissues (28,29). BMMSCs can also secrete soluble cytokines through paracrine mechanisms to reduce inflammatory reactions and enhance reparative effects (30,31). BMMSCs exert inhibitory effects on the rejection response following small bowel transplantation, and reduce intestinal damage (9). HO-1 gene modification can enhance the ability of BMMSCs to tolerate hypoxia-reoxygenation injury, and enhance BMMSC viability and proliferation (4,5,13,14). Chemokine receptor CXCR3 is typically expressed in the parenchyma cells of diseased organs and activated inflammatory cells (15). Upon binding specifically to their ligands, CXCR3 receptors induce the chemotaxis of lymphocytes to damaged sites (16,17,32), and further activate lymphocytes to produce a pro-inflammatory response through the regulation of the T helper cell signaling pathway (33). Due to the specific binding of the receptor to its ligand, BMMSCs that overexpress the CXCR3 gene are able to compete with such activated lymphocytes for the CXCR3 ligand. This allows for a large number of activated lymphocytes to remain unbound to the CXCR3 receptor, thereby inhibiting the positive feedback mechanism required for a continued effector response. Additional lymphocytes cannot be recruited to the damaged sites, leading to the reduced secretion of inflammatory cytokines and therefore, reduced cellular injury. Our previous study demonstrated that the efficiency and survival duration of BMMSCs were significantly improved following modification by the HO-1 and CXCR3 genes in animal models of small bowel transplantation (18). However, the mechanism by which BMMSCs repair damaged intestinal cells remains to be elucidated. Therefore, the present study used an *ex vivo* model of damaged intestinal epithelial cells to model *in vivo* responses.

The experimental model used standard BMMSCs as previously described (34,35). Following transfection with the HO-1 gene and/or CXCR3 gene, the BMMSCs maintained their functionality, and the viability assessment confirmed that the HO-1 gene and CXCR3 gene did not have any toxic effects. In the rejection model of small bowel transplantation, TNF-α increased significantly (9), inducing damage to the intestinal epithelial cells (36); thus, the present study used undifferentiated IEC-6 cells to simulate the *in vivo* intestinal mucosal environment (24). The results demonstrated that the expression of the tight junction protein (ZO-1) in IEC-6 cells treated with TNF-α was significantly decreased and the number of apoptotic cells was significantly increased.

This finding indicates that the establishment of an *in vitro* model of damaged intestinal epithelial cells using TNF-α and IEC-6 cells had been successful. The BMMSCs increased the expression of ZO-1 and the proliferation of IEC-6 cells, and decreased IEC-6 apoptosis. Further investigation revealed that the protective effects of Ad-(CXCR3 + HO)/MSCs on damaged intestinal epithelial cells was more marked than that of the Ad-HO/MSCs and BMMSCs, which was consistent with the conclusions of the *in vivo* model (18).

The chemokine receptor, CXCR3, is expressed on the surface of activated lymphocytes *in vivo* (15). Therefore, when the CXCR3 receptor specifically binds with its ligand, CXCR3-expressing cells can be recruited into the site of injury (16,17). CXCR3-overexpressing BMMSCs compete with activated T lymphocytes for the CXCR3 ligand, inhibiting further activation of T lymphocytes and significantly reducing the inflammatory response (33). CD25 and CD71 are characteristic surface markers of lymphocyte activation, exhibit low expression during steady-state conditions and become expressed at high levels following activation (37-39). IL-2 (40) and IFN-γ (41) are sensitive cytokines that can reflect the activity of T cells. The results of the present study showed that the expression levels of $CD3^+CD25^+$ and $CD3^+CD71^+$ were significantly decreased and those of IL-2 and IFN-γ were significantly reduced following repair by Ad-CXCR3/MSCs or Ad-(CXCR3 + HO)/MSCs. This finding confirmed that CXCR3 gene-modified BMMSCs are important in the inhibition of lymphocyte activation. In addition, CXCR3 gene-modified BMMSCs demonstrated the highest level of mobility and chemotaxis, which suggested that an increased number of BMMSCs arriving to the damaged site and decreased activity of T lymphocytes was the major cause of the enhanced reparative effects. Therefore, the specific mechanism by which this occurs warrants further investigation.

Studies have shown that the p38-MAPK pathway serves an important role in the sequence of events inflammatory responses caused by trauma (19), infection (20) and ischemia-reperfusion (21). MLK3 and MKK3 are the main upstream molecules of the p38-MAPK pathway, and can phosphorylate the p38-MAPK protein following activation. The phosphorylation of p38-MAPK influences the activation of the downstream molecules, ATF2, CHOP10 and MEF2C, further affecting the proliferation, differentiation and cytokine synthesis of cells (42,43). In the present study, the expression of p-p38 MAPK protein in damaged IEC-6 cells was significantly increased, suggesting that this signaling pathway was activated. However, the expression of the upstream molecules p-MLK3 and p-MKK3 in the p38-MAPK pathway of the different groups was not statistically significant, indicating that the BMMSCs did not have an effect on the upstream molecules in the p38-MAPK pathway. When treated with a p38 inhibitor or BMMSCs, the expression of p-p38 MAPK significantly decreased, indicating that both the inhibitor and BMMSCs inhibited the phosphorylation of p38 MAPK. The downstream molecules p-ATF2, p-CHOP10 and p-MEF2C in the p38-MAPK pathway were significantly decreased in all groups treated with BMMSCs, and the decreases in the Ad-CXCR3/MSCs and Ad-(CXCR3 + HO)/MSCs treatment groups were the most marked. These results suggest that p38-MAPK and the downstream molecules of the p38-MAPK pathway are involved in the repair of damaged intestinal epithelial cells by BMMSCs.

ATF2 (44,45), CHOP-10 (46-48) and MEF2C (49,50) have physiological roles in the control of cellular growth, differentiation and apoptosis (44-50). Their target molecules include PCNA, apoptotic bodies and ZO-1 protein. The present study demonstrated that activation of the p38-MAPK signaling pathway reduced the expression of ZO-1 and PCNA, and significantly increased apoptosis. When signaling was inhibited by inhibitors or BMMSCs, the expression levels of ZO-1 and PCNA were increased, and apoptosis was decreased. This effect was the most marked in the Ad-CXCR3/MSCs and Ad-(CXCR3 + HO)/MSCs groups. These results indicate that the downstream constituents of the p38-MAPK pathway are involved in the repair of damaged intestinal epithelial cells by CXCR3 and HO-1 gene-modified BMMSCs *in vitro*.

In addition, it was found that the effects of Ad-CXCR3/MSCs were more marked than those of simple MSCs on POD 7 following small bowel transplantation in the preliminary experiment (18), suggesting that Ad-CXCR3 was associated with significant chemotactic effects. The median survival rate and pathological changes of the rats in the Ad-CXCR3/MSCs group and the MSCs group were similar on day 7 following small bowel transplantation (Figs. S2 and S3). As the present study focused on elucidating the role of the double gene-modified BMMSCs, six groups were assessed, not including the Ad-CXCR3/MSCs group. p-38 MAPK-related molecules were assessed on day 7 following small bowel transplantation in different treatment groups of an *in vivo* rejection model (NSBT, IsoT, NS, MSCs, Ad-HO-1/MSC, and Ad-(CXCR3 + HO)/MSCs). Compared with the BMMSCs, Ad-(CXCR3 + HO)/MSCs significantly decreased the expression of p-38-MAPK, and the downstream molecules p-ATF2, p-CHOP-10 and p-MEF2C of the p-38-MAPK pathway. the expression of target molecules (e.g., decreased apoptosis) were also reduced (18), whereas the expression levels of PCNA and ZO-1 were increased. The expression of upstream molecules did not differ between the various treatment groups, which verified the results of the *in vitro* experiments.

The effects of Ad-HO/MSCs in an *ex vivo* model were similar to that of BMMSCs, whereas the effects of Ad-HO/MSCs were more marked than BMMSCs in the rat model of small bowel transplantation, which may be associated with the action time of the different stem cells. As lymphocytes were added in the experimental groups, their survival rate declined after 24 h. Therefore, the investigation was limited to 24 h *in vitro*, when the stem cells remained highly active; however, the HO-1 gene may not have been fully effective. Using a rat model of small bowel transplantation, the results were analyzed 7 days following small bowel transplantation, when the activity of BMMSCs was significantly reduced and that of Ad-HO/MSCs remained high. The CXCR3 gene enhanced the chemotactic ability of the BMMSCs, enabling a higher number of stem cells to reach damaged sites more rapidly to exert reparative effects. The gene expression of CXCR3 only exhibited a chemotactic effect in the absence of lymphocyte involvement. However, in the presence of lymphocytes, CXCR3-gene modified BMMSCs were able to compete with lymphocytes for the CXCR3 ligands. This inhibited lymphocyte activation,

reduced the secretion of inflammatory cytokines and further decreased the extent of cellular damage. The process of stem cell reparative effects is complex, which may involve the combined action of multiple pathways. However, only the p38-MAPK pathway was involved in transplantation repair in the present study. Therefore, as the effects of stem cells have not been comprehensively examined, future investigations aim to examine whether Wnt/β-catenin and other pathways are also involved in regeneration and reparation.

In conclusion, CXCR3 and HO-1 double gene-modified BMMSCs and CXCR3 gene-modified BMMSCs demonstrated significant reparative effects on damaged intestinal epithelial cells *in vitro*. The gene expression of CXCR3 enhanced the chemotactic ability of BMMSCs, which induced the early and rapid recruitment of BMMSCs overexpressing this gene to the damaged site. It was also demonstrated that BMMSCs exert this effect via p38-MAPK pathway. Taken together, these findings provide an experimental basis for the dual gene therapy of stem cells.

Acknowledgements

Not applicable.

Funding

The present study was supported by the National Natural Science Foundation of China (grant nos. 81670574, 81441022 and 81270528); the Tianjin Clinical Research Center for Organ Transplantation Project (15ZXLCSY00070) and the Natural Science Foundation of Tianjin, China (grant nos. 08JCYBJC08400, 11JCZDJC27800 and 12JCZDJC25200).

Availability of data and materials

All data generated or analyzed during this study are included in this published article.

Authors' contributions

MY and ZS performed the research, analyzed the data, and wrote and revised the manuscript; MY, WZ and LY performed the research; WZ participated in analyzing the data; HS designed the research, participated in revision of the manuscript. All authors have read and approved the final manuscript.

Ethics approval and consent to participate

All experiments involving animals followed the experimental animal ethical regulations, and were approved by the Ethics Committee of Tianjin First Central Hospital.

Patient consent for publication

Not applicable.

Competing interests

The authors declare that they have no competing interests.

References

1. Ruiz P, Kato T and Tzakis A: Current status of transplantation of the small intestine. Transplantation 83: 1-6, 2007.
2. Koo J, Dawson DW, Dry S, French SW, Naini BV and Wang HL: Allograft biopsy findings in patients with small bowel transplantation. Clin Transplant 30: 1433-1439, 2016.
3. Libby P and Pober JS: Chronic rejection. Immunity 14: 387-397, 2001.
4. Yang Y, Song HL, Zhang W, Wu BJ, Fu NN, Dong C and Shen ZY: Hemeoxygenase-1-transduced bone marrow mesenchymal stem cells in reducing acute rejection and improving small bowel transplantation outcomes in rats. Stem Cell Res Ther 7: 164, 2016.
5. Wu B, Song HL, Yang Y, Yin ML, Zhang BY, Cao Y, Dong C and Shen ZY: Improvement of liver transplantation outcome by heme oxygenase-1-transduced bone marrow mesenchymal stem cells in rats. Stem Cells Int 2016: 9235073, 2016.
6. Schu S, Nosov M, O'Flynn L, Shaw G, Treacy O, Barry F, Murphy M, O'Brien T and Ritter T: Immunogenicity of allogeneic mesenchymal stem cells. J Cell Mol Med 16: 2094-2103, 2012.
7. De Miguel MP, Fuentes-Julian S, Blazquez-Martinez A, Pascual CY, Aller MA, Arias J and Arnalich-Montiel F: Immunosuppressive properties of mesenchymal stem cells: Advances and applications. Curr Mol Med 12: 574-591, 2012.
8. Barry FP and Murphy JM: Mesenchymal stem cells: Clinical applications and biological characterization. Int J Biochem Cell Biol 36: 568-584, 2004.
9. Yang Y, Song HL, Zhang W, Wu BJ, Fu NN, Zheng WP, Dong C and Shen ZY: Reduction of acute rejection by bone marrow mesenchymal stem cells during rat small bowel transplantation. Plos One 9: e114528, 2014.
10. Hodgkinson CP, Gomez JA, Mirotsou M and Dzau VJ: Genetic engineering of mesenchymal stem cells and its application in human disease therapy. Hum Gene Ther 21: 1513-1526, 2010.
11. Freyman T, Polin G, Osman H, Crary J, Lu M, Cheng L, Palasis M and Wilensky RL: A quantitative, randomized study evaluating three methods of mesenchymal stem cell delivery following myocardial infarction. Eur Heart J 27: 1114-1122, 2006.
12. Yamashita K, Ollinger R, McDaid J, Sakahama H, Wang H, Tyagi S, Csizmadia E, Smith NR, Soares MP and Bach FH: Heme oxygenase-1 is essential for and promotes tolerance to transplanted organs. FASEB J 20: 776-778, 2006.
13. Vanella L, Kim DH, Asprinio D, Peterson SJ, Barbagallo I, Vanella A, Goldstein D, Ikehara S, Kappas A and Abraham NG: HO-1 expression increases mesenchymal stem cell-derived osteoblasts but decreases adipocyte lineage. Bone 46: 236-243, 2010.
14. Zeng B, Lin G, Ren X, Zhang Y and Chen H: Over-expression of HO-1 on mesenchymal stem cells promotes angiogenesis and improves myocardial function in infarcted myocardium. J Biomed Sci 17: 80, 2010.
15. Jenh CH, Cox MA, Cui L, Reich EP, Sullivan L, Chen SC, Kinsley D, Qian S, Kim SH, Rosenblum S, *et al*: A selective and potent CXCR3 antagonist SCH 546738 attenuates the development of autoimmune diseases and delays graft rejection. BMC Immunol 13: 2, 2012.
16. Agostini C, Calabrese F, Rea F, Facco M, Tosoni A, Loy M, Binotto G, Valente M, Trentin L and Semenzato G: CXCR3 and its ligand CXCL10 are expressed by inflammatory cells infiltrating lung allografts and mediate chemotaxis of T cells at sites of rejection. Am J Pathol 158: 1703-1711, 2001.
17. Hancock WW, Wang L, Ye Q, Han R and Lee I: Chemokines and their receptors as markers of allograft rejection and targets for immunosuppression. Curr Opin Immunol 15: 479-486, 2003.
18. Yin ML, Song HL, Yang Y, Zheng WP, Liu T and Shen ZY: Effect of CXCR3/HO-1 genes modified bone marrow mesenchymal stem cells on small bowel transplant rejection. World J Gastroenterol 23: 4016-4038, 2017.
19. Chu W, Li M, Li F, Hu R, Chen Z, Lin J and Feng H: Immediate splenectomy down-regulates the MAPK-NF-κB signaling pathway in rat brain after severe traumatic brain injury. J Trauma Acute Care Surg 74: 1446-1453, 2013.
20. Wu H, Wang G, Li S, Zhang M, Li H and Wang K: TNF-α-mediated-p38-dependent signaling pathway contributes to myocyte apoptosis in rats subjected to surgical trauma. Cell Physiol Biochem 35: 1454-1466, 2015.
21. Dai J, Gu L, Su Y, Wang Q, Zhao Y, Chen X, Deng H, Li W, Wang G and Li K: Inhibition of curcumin on influenza A virus infection and influenzal pneumonia via oxidative stress, TLR2/4, p38/JNK MAPK and NF-κB pathways. Int Immunopharmacol 54: 177-187, 2017.

22. Khan SI, Malhotra RK, Rani N, Sahu AK, Tomar A, Garg S, Nag TC, Ray R, Ojha S, Arya DS and Bhatia J: Febuxostat modulates MAPK/NF-κBp65/TNF-α signaling in cardiac ischemia-reperfusion injury. Oxid Med Cell Longev 2017: 8095825, 2017.
23. Cuadrado A and Nebreda AR: Mechanisms and functions of p38 MAPK signalling. Biochem J 429: 403-417, 2010.
24. Gao JH, Guo LJ, Huang ZY, Rao JN and Tang CW: Roles of cellular polyamines in mucosal healing in the gastrointestinal tract. J Physiol Pharmacol 64: 681-693, 2013.
25. Liu T, Fu NN, Song HL, Wang YL, Wu BJ and Shen ZY: Suppression of microRNA-203 improves survival of rat bone marrow mesenchymal stem cells through enhancing PI3K-induced cellular activation. IUBMB Life 66: 220-227, 2014.
26. Cao Y, Wu BJ, Zheng WP, Yin ML, Liu T and Song HL: Effect of heme oxygenase-1 transduced bone marrow mesenchymal stem cells on damaged intestinal epithelial cells in vitro. Cell Biol Int 41: 726-738, 2017.
27. Livak KJ and Schmittgen TD: Analysis of relative gene expression data using real-time quantitative PCR and the 2(-Delta Delta C(T)) method. Methods 25: 402-408, 2001.
28. Ho MS, Mei SH and Stewart DJ: The immunomodulatory and therapeutic effects of mesenchymal stromal cells for acute lung Injury and sepsis. J Cell Physiol 230: 2606-2617, 2015.
29. Chen J, Li C and Chen L: The role of microvesicles derived from mesenchymal stem cells in lung diseases. Biomed Res Int 2015: 985814, 2015.
30. English K: Mechanisms of mesenchymal stromal cell immunomodulation. Immunol Cell Biol 91: 19-26, 2013.
31. Le Blanc K and Mougiakakos D: Multipotent mesenchymal stromal cells and the innate immune system. Nat Rev Immunol 12: 383-396, 2012.
32. Singh AK, Arya RK, Trivedi AK, Sanyal S, Baral R, Dormond O, Briscoe DM and Datta D: Chemokine receptor trio: CXCR3, CXCR4 and CXCR7 crosstalk via CXCL11 and CXCL12. Cytokine Growth Factor Rev 24: 41-49, 2013.
33. Billottet C, Quemener C and Bikfalvi A: CXCR3, a double-edged sword in tumor progression and angiogenesis. Biochim Biophys Acta 1836: 287-295, 2013.
34. Morikawa S, Mabuchi Y, Kubota Y, Nagai Y, Niibe K, Hiratsu E, Suzuki S, Miyauchi-Hara C, Nagoshi N, Sunabori T, *et al*: Prospective identification, isolation, and systemic transplantation of multipotent mesenchymal stem cells in murine bone marrow. J Exp Med 206: 2483-2496, 2009.
35. Song K, Huang M, Shi Q, Du T and Cao Y: Cultivation and identification of rat bone marrow-derived mesenchymal stem cells. Mol Med Rep 10: 755-760, 2014.
36. Zheng XK, Liu CX, Zhai YY, Li LL, Wang XL and Feng WS: Protection effect of amentoflavone in selaginella tamariscina against TNF-alpha-induced vascular injury of endothelial cells. Yao Xue Xue Bao 48: 1503-1509, 2013 (In Chinese).
37. Le Blanc K, Rasmusson I, Götherström C, Seidel C, Sundberg B, Sundin M, Rosendahl K, Tammik C and Ringdén O: Mesenchymal stem cells inhibit the expression of CD25 (interleukin-2 receptor) and CD38 on phytohaemagglutinin-activated lymphocytes. Scand J Immunol 60: 307-315, 2004.
38. Shipkova M and Wieland E: Surface markers of lymphocyte activation and markers of cell proliferation. Clin Chim Acta 413: 1338-1349, 2012.
39. Daniels TR, Delgado T, Rodriguez JA, Helguera G and Penichet ML: The transferrin receptor part I: Biology and targeting with cytotoxic antibodies for the treatment of cancer. Clin Immunol 121: 144-158, 2006.
40. Elhaik Goldman S, Dotan S, Talias A, Lilo A, Azriel S, Malka I, Portnoi M, Ohayon A, Kafka D, Ellis R, *et al*: Streptococcus pneumoniae fructose-1,6-bisphosphate aldolase, a protein vaccine candidate, elicits Th1/Th2/Th17-type cytokine responses in mice. Int J Mol Med 37: 1127-1138, 2016.
41. Xiang RL, Mei M, Su YC, Li L, Wang JY and Wu LL: Visfatin protects rat pancreatic β-cells against IFN-γ-Induced apoptosis through AMPK and ERK1/2 signaling pathways. Biomed Environ Sci 28: 169-177, 2015.
42. Duarte S, Shen XD, Fondevila C, Busuttil RW and Coito AJ: Fibronectin-α4β1 interactions in hepatic cold ischemia and reperfusion injury: Regulation of MMP-9 and MT1-MMP via the p38 MAPK pathway. Am J Transplant 12: 2689-2699, 2012.
43. Peng S, Hang N, Liu W, Guo W, Jiang C, Yang X, Xu Q and Sun Y: Andrographolide sulfonate ameliorates lipopolysaccharide-induced acute lung injury in mice by down-regulating MAPK and NF-κB pathways. Acta Pharm Sin B 6: 205-211, 2016.
44. Lopez-Bergami P, Lau E and Ronai Z: Emerging roles of ATF2 and the dynamic AP1 network in cancer. Nat Rev Cancer 10: 65-76, 2010.
45. Lau E and Ronai ZA: ATF2 - at the crossroad of nuclear and cytosolic functions. J Cell Sci 125: 2815-2824, 2012.
46. Todd DJ, Lee AH and Glimcher LH: The endoplasmic reticulum stress response in immunity and autoimmunity. Nat Rev Immunol 8: 663-674, 2008.
47. Li Y, Guo Y, Tang J, Jiang J and Chen Z: New insights into the roles of CHOP-induced apoptosis in ER stress. Acta Biochim Biophys Sin (Shanghai) 47: 146-147, 2015.
48. He J, Wang C, Sun Y, Lu B, Cui J, Dong N, Zhang M, Liu Y and Yu B: Exendin-4 protects bone marrow-derived mesenchymal stem cells against oxygen/glucose and serum deprivation-induced apoptosis through the activation of the cAMP/PKA signaling pathway and the attenuation of ER stress. Int J Mol Med 37: 889-900, 2016.
49. Shi GX, Han J and Andres DA: Rin GTPase couples nerve growth factor signaling to p38 and b-Raf/ERK pathways to promote neuronal differentiation. J Biol Chem 280: 37599-37609, 2005.
50. Wu J, Kubota J, Hirayama J, Nagai Y, Nishina S, Yokoi T, Asaoka Y, Seo J, Shimizu N, Kajiho H, *et al*: P38 mitogen-activated protein kinase controls a switch between cardiomyocyte and neuronal commitment of murine embryonic stem cells by activating myocyte enhancer factor 2C-dependent bone morphogenetic protein 2 transcription. Stem Cells Dev 19: 1723-1734, 2010.